Proteome analysis in dystrophic mdx mouse muscle reveals a drastic alteration of key metabolic and contractile proteins after chronic

Proteome analysis in dystrophic mdx mouse muscle reveals a drastic alteration of Key Metabolic and Contractile Proteins after chronic exercise and the potential modulation by anti-oxidant compounds

Tania Gamberi[*], Tania Fiaschi[*], Elisa Valocchia[*], Alessandra Modesti[*], Paola Mantuano [≠], Jean-Francois Rolland [§], Francesca Sanarica [≠], Annamaria De Luca[≠ł] and Francesca Magherini[*ł]

*Department of Experimental and Clinical Biomedical Sciences "Mario Serio", University of Florence, Florence, Italy

[≠] Section of Pharmacology, Department of Pharmacy & Drug Sciences, University of Bari "Aldo Moro", Bari, Italy

[§]Axxam s.p.a., Calco (Milan) Italy

[ł] These two co-authors contributed equally to this work

Corresponding authors:

[ł]Annamaria de Luca

Sezione di Farmacologia, Dipartimento di Farmacia–Scienze del Farmaco, Università Degli Studi di Bari "Aldo Moro," Bari, Italy

+39 080 5442245

annamaria.deluca@uniba.it

[ł] Francesca Magherini

Dipartimento di Scienze Biomediche Sperimentali e Cliniche "Mario Serio" Università degli Studi di Firenze, Italia

Viale Morgagni 50, Firenze

+390552751237

francesca.magherini@unifi.it

Abstract

Weakness and fatigability are typical features of Duchenne muscular dystrophy patients and are aggravated in dystrophic mdx mice by chronic treadmill exercise. In the present study, we describe, the pattern of differentially abundant spots that is associated to the worsening of dystrophy phenotype induced by chronic exercise. Our proteomic analysis pointed out 34 protein spots with different abundance between sedentary and exercised mdx mice. These proteins belong mostly to glucose metabolism, energy production and sarcomere structure categories. Interestingly exercise induced an increase of typical fast twitch fiber proteins (Troponin T fast skeletal muscle, Troponin I fast skeletal muscle and Myozenin-1) combined with an increase of several glycolytic enzymes. Concerning energy transfer, Adenylate kinase, showed a marked decrease when compared with non-exercised mdx. The decline of this enzyme correlates with increased Creatin kinase enzyme, suggesting that a compensatory energy metabolism mechanism could be activated in mdx mouse skeletal muscle following exercise. In addition, we analysed muscles from exercised mdx mice treated with two natural anti-oxidant compounds, apocynin and taurine, that in our previous study, were proved to be beneficial on some pathology related parameters, and we showed that these compounds can counteract exercise-induced changes in the abundance of several proteins.

Keywords: Duchenne muscular dystrophy, mdx mice, two dimensional gel electrophoresis, mass spectrometry, proteomics, taurine, apocynin.

1. Introduction

Duchenne Muscular Dystrophy (DMD) is a severe, X-chromosome linked disease inherited muscle disorder caused by the absence of functional dystrophin protein. It affects 1 in 5000 boys worldwide; no definitive treatment for this disease is available yet. DMD is characterized by muscle membrane fragility, progressive myofiber death and replacement of skeletal muscle by fibrous and connective tissue (due to failed regeneration). This results in extensive wasting, weakness and loss of muscle function leading to premature death.

The dystrophin-deficient mdx mouse is the most common animal model for DMD [1], and it is characterized by a nonsense mutation in exon 23 of the dystrophin gene. The mdx mice phenotype of the disorder is milder than in human sufferers. This difference arises from differences in size, mechanical loading and lifespan [2]. These mice present an acute onset of pathology around 3-4 weeks of age, that is reduced to a chronic low level of damage by 8 weeks and persists throughout life [3]. Compared to DMD patients, mdx mouse muscles show less accumulation of connective and adipose tissue and are characterized by a better recover from the wasting. In fact, although the necrotic process persists throughout their life, the regenerative capacity does not decline until an advanced age (around one year) [4].

Since regular exercise has a plethora of positive effects on health and muscle performance, exercise has been proposed as treatment for DMD, but this recommendation has not been unanimously accepted because inappropriate exercise damages dystrophic muscles [5,6]. The establishment of the exact boundary line between a proper and unsuitable exercise is challenging. The effect of exercise in mdx mouse model has been largely used for basically three purposes: i) assessing the physical capacities of the mice, ii) investigating the effects of training on dystrophic muscles, iii) worsening the phenotype in order to assess the effects of a drug [5]. In the context of worsen the mild dystrophic phenotype of mdx mice, various models of exercise-induced muscle damage,

including forced wheel or treadmill running, and swimming, were used. These protocols can mimic the muscle progressive damage observed in humans, can allow studying the effects of inadequate training on dystrophic muscles and have been largely used to assess the ability of a drug to reduce the damage induced by exercise [3,5]. Several proteomic studies, comparing wild type and mdx muscles were performed [7–12], however only few investigated the effect of exercise [13,14]. In particular, these studies were focused on the beneficial effect of a low intensity exercise, while the effect of high intensity protocols has never been investigated by a proteomic approach. In a previous study, we analyzed how a chronic protocol of treadmill exercise affects the in vivo performance and the expression of specific molecules involved in muscle damage and regeneration in mdx mice [15]. We demonstrated that this protocol reduces functional performance in vivo in mdx mice. In parallel, we demonstrated that exercised mdx mice showed changes in expression genes indicating a failure in mechanical metabolic coupling. In particular, we observed an impaired ability of adaptation to exercise of protective metabolic oxidative pathways, while the gene expression of proteins involved in damaging signals, such as oxidative stress and inflammation, remains upregulated. Importantly, no change was detected in wild-type mice, the protocol being too mild to induce training effects in healthy animals [15]. The more severe phenotype induced by chronic exercise is useful to test the beneficial effects of drugs and natural compounds, among which anti-oxidant and anti-inflammatory drugs [16-18]. In the present study, we describe, for the first time, the pattern of differentially abundant spots that is associated to the worsening of dystrophy phenotype induced by chronic exercise. Our investigation includes the protein profile in tibialis anterior muscle of wild type, mdx mice and mdx mice undergoing a standard 4 weeks' protocol of exercise on treadmill. In particular, we focused our attention to changes induced by exercise in the mdx phenotype, showing significant alteration of several metabolic pathways including glucose one, as well as sarcomere structure organization. In addition, we also analyzed muscle from exercised mdx mice treated with two natural anti-oxidant compounds, apocynin and taurine, proved to be beneficial on some pathology related parameters [16], in order to assess, at

proteomic level, if the exercise and pathology related changes could be counteracted by these compounds.

2. Materials and Methods

2.1 Animal model and exercise

The present study was performed using the hind limb muscle samples of experimental mice groups previously used [16,19]. In particular, muscle samples used in this study are referred to the following mice and experimental groups: male mdx mice (C57BL/10ScSn-Dmdmdx/J from Jackson Laboratories) divided in sedentary mdx (mdx) mice or exercised mdx (mdx exe) mice, mdx exercised mice treated with taurine (mdx exe tau) or apocynin (mdx exe apo) and C57/BL wild-type (wt) mice. The age of all mice at the beginning of the study was 4-5 weeks while muscle sampling was performed at 8-10 weeks of age. The training protocol consisted of a 30 min running on a horizontal treadmill (Columbus Instruments, USA) at 12 m/min, twice a week (keeping a constant interval of 2–3 days between each trial), for 4 weeks. The doses of taurine and apocynin were 1 g/kg (orally) and 38 mg/kg (1.5 mmol/l in drinking water) respectively. The treatment started one day before the beginning of the exercise protocol, lasted at least 4 weeks and continued until the day of sacrifice. A group of age-matched male wild-type mice (C57BL/10) has also been used as control. The animals were sacrificed after 48-72 hours after the last exercise session to avoid acute effects of exercise to be detected [19]. Muscles were removed, immediately frozen in liquid nitrogen and stored at −80 °C until use for biochemical evaluations. The animals used in this proteomic study were 5 for each group.

2.2 Muscle sample preparation and two-dimensional gel electrophoresis

Muscle protein extracts were prepared as previously described [20]. Briefly, frozen muscles were ground in dry ice in a cooled mortar, suspended in lysis buffer (50 mM Tris–HCl pH 7.0, 150 mM,

NaCl, 2 mM EGTA, 100 mM NaF, 1% (v/v) NP-40, 0.5% (w/v), deoxycholate, 0.1% (w/v) SDS containing a cocktail of protease inhibitors (Sigma) and solubilized by sonication on ice.

After centrifugation (8000 RCF, for 5 m) proteins were precipitated following a chloroform/methanol protocol [21] and suspended in 8 M urea, 4% (w/v) CHAPS, 50 mM DTT. Protein samples (60 μg for silver stained gels and 700 μg for preparative gels) were separated on 18-cm immobilized pH gradient (IPG) strips (pH 3-10 NL) on PROTEAN® i12™ IEF System (BIO-RAD). In particular, the strips were actively rehydrated (at 50V), for 14 hours, in the presence of sample in rehydration solution (8 M urea, 2% (w/v) CHAPS, 0.5% (w/v) DTE) supplemented with 0.5% (v/v) carrier ampholyte (Bio-Rad) and a trace of bromophenol blue. The strips were then focused at 16°C according to the following electrical conditions: 250 V for 20 m (rapid), from 250V to 8000V for 1 h, 8000V until a total of 43000 V/h was reached, with a limiting current of 50 μA/strip. Analytical gels were stained with ammoniacal silver nitrate as previously described [22]; MS-preparative gels were stained with colloidal Coomassie blu silver [23].

2.3 Image analysis and statistics

In this study we used 5 animals for group (biological replicates) and for each animal two 2DE gels were carried out (technical replicates), so that, in total 50 gels were analyzed. Silver-stained gels were scanned using the Epson expression 1680 PRO scanner. The gel images were saved with a resolution of 300 dpi and in 16-bit TIFF format. Image analysis was carried out using the Progenesis SameSpots software v4.0 (Nonlinear Dynamics, UK), which allows spot detection, background subtraction and protein spot volume quantification. The gel image showing the highest number of spots and the best protein pattern was chosen as the reference image and its spots were then matched across all gels. This reference image was used to quantify and normalize the spot volumes. The spot volumes were normalized in each gel as relative volume (volume percentage), by dividing the raw quantity of each spot by the total quantity of all the spots included in the reference gel. Statistical analysis was performed using default parameters of the Progenesis SameSpots Stat module. The log10-normalized spot volume was used for the analysis as the log transformation

improves normality [24]. The univariate data analysis was performed as one-way ANOVA on each spot individually. Then, a multivariate statistic was applied on all the ANOVA p-values by the False Discovery Rate (FDR) correction method. Moreover, we performed a power analysis to assess the number of sample replicates that need to be analyzed in order to confidently discover differentially abundant proteins. The accepted power threshold is ≥ 0.8.62 The differences were considered significant for the spots having a corrected p-value (FDR) ≤0.05 and a power ≥0.8. These spots were subjected to mass spectrometry analysis. Tukey correction for multiple comparison was performed with GraphPad Prism v6.0 software in order to find out the significant differences between groups.

2.4 Mass spectrometry (MS) protein identification

Electrophoretic spots were manually excised, destained, and acetonitrile dehydrated. A trypsin solution (0.25 mg/ml) in 50 mM ammonium bicarbonate was added for in-gel protein digestion by overnight incubation at 37 °C. Solutions containing digested peptides were recovered and 20 µL of 1% TFA 50% ACN were added to each spot and sonicated for 10 minutes to maximize peptide recovery. At the end, for each spot, all recovered peptide solutions were combined and concentrated. From each protein digest, 0.75 µL were spotted onto the MALDI target and allowed to air dry at room temperature. Then, 0.75 µL of matrix solution (saturated solution of a-cyano-4-hydroxy- cinnamic acid in 50% (v/v) acetonitrile and 0.5% (v/v) TFA) was applied to the sample and crystallized by air drying at room temperature for 5 min. Protein identification was carried out by peptide mass fingerprinting (PMF) on an Ultraflex III MALDI- TOF/TOF mass spectrometer (Bruker Daltonics) equipped with a 200 Hz smartbeamt I laser. MS analysis was performed in the positive reflector mode according to defined parameters, as follows: 80 ns of delay; ion source 1: 25 kV; ion source 2: 21.75 kV; lens voltage: 9.50 kV; reflector voltage: 26.30 kV; and reflector 2 voltage: 14.00 kV. The applied laser wavelength and frequency were 353 nm and 100 Hz, respectively, and the percentage was set to 46%. Final mass spectra were produced by averaging 1500 laser shots targeting five different positions within the spot. Spectra were acquired

automatically and the Flex Analysis software version 3.0 (Bruker) was used for their analysis and for the assignment of the peaks. The applied software generated a list of peaks up to 200, using a signal-to-noise ratio of 3 as the threshold for peak acceptance. Recorded spectra were calibrated using, as the internal standard, peptides arising from trypsin auto-proteolysis. The mass lists were filtered for contaminant removal: mass matrix- related ions, trypsin auto-lysis and keratin peaks. Protein identification by Peptide Mass Fingerprint search was established using MASCOT search engine version 2.1 (Matrix Science, London, UK, http://www.matrixscience.com) through the UniProtKB database (accession December 2016) (http://www.uniprot.org/). Taxonomy was limited to *Mus musculus,* a mass tolerance of 100 ppm was allowed, and the number of accepted missed cleavage sites was set to one. Alkylation of cysteine by carbamidomethylation was considered a fixed modification, while oxidation of methionine was considered as a possible modification. The criteria used to accept identifications included the extent of sequence coverage, the number of matched peptides, and a probabilistic score of $p \leq 0.05$.

2.5 Bioinformatic functional analysis

Identified proteins were used as input list in order to obtain a categorization and an over-representation analysis (ORA) using the Webgestalt online tool ("WEB-based GEne SeT AnaLysis Toolkit") (http://www.webgestalt.org/) against GeneOntology (GO) and WikiPathway [25]. The statistics performed in the over-representation analysis (ORA) dealt with the p-value obtained from the Fisher exact test followed by the p-value adjusted for multiple testing by the Benjamini-Hochberg correction.

2.6 Western blot analysis

For 1DE, protein extracts were separated by 12% SDSPAGE and transferred onto a PVDF membrane (Millipore). The relative abundance of Aldolase, Enolase, Triosephosphate isomerase, Actin, PGC-1α, Sirt1, proteins was assessed by Western blot with appropriate antibodies (Aldolase, Enolase, Triosephosphate isomerase Actin, PGC-1α antibodies from Santa Cruz Biotechnology; Sirt1 antibodies from Cell Signalling). Oxphos complexes were analysed, by immunoblot, using

Total OXPHOS Rodent WB Antibody Cocktail (Abcam). For quantification, the blots were subjected to densitometric analysis performed using ImageJ image processing program [26]. For the normalization, PVDF membranes were stained with Coomassie brilliant blue R-250 and the intensity of the each immunostained band was normalized on protein staining of the corresponding whole lane. Statistical analysis of the data was performed by Student's t-test using GraphPad Prism software; p-values ≤ 0.05 were considered statistically significant.

3. Results and Discussion

3.1 Overview of overall proteomic analysis

In order to better understand how exercise impacted protein abundance in mdx mice, proteins from tibialis anterior (TA) of sedentary mdx (mdx) and mdx mice after four weeks of exercise (mdx exe) were separated by 2DE and protein profile were analyzed using Progenesis SameSpot software v4.0 (Nonlinear Dynamics, UK). We also included in this analysis TA muscle proteins extracted from wild type mice (wt), that was considered as referring phenotype, and mdx exercised animals treated with taurine (mdx exe tau) and apocynin (mdx exe apo) as previously described [16]. The 2DE gel images were analysed by the software using default parameters. After automatic spot detection, an average of about 970 protein spots was detected in each gel (Figure 1). The computational 2DE gel image analysis pointed out 120 spots showing different abundance (ANOVA p-value ≤ 0.05). In addition to univariate analysis (ANOVA-test), multivariate analyses (q-value, PCA and power analysis) were performed to explore categories of differential protein level. To reduce the expected level of false positive, we performed a statistical analysis on the ANOVA p-values, by applying the false discovery rate correction method known as q-value. A statistically significant q-value (≤ 0.05) was found for 112 protein spots. Moreover, we calculated the power of our statistical analysis: in our experiments, we achieved a target power of 87% confirming that the number of sample replicates used was appropriate. The abundance of the spots was considered statistically different

when associated with a q-value ≤ 0.05 and a power ≥0.8. To obtain an overview of the proteomic data for overall trends in all groups, PCA was performed. Gels were grouped according to the variance of protein spot abundance. In PCA biplot, each point describes the collective expression profiles of one sample and plot demonstrates consistent reproducibility between the replicate samples within each group. The PCA biplot, shown in Figure 2, reveals two distinct main protein profile groups corresponding to: i) mdx and wt (red circle), ii) mdx exe and mdx exe treated with apocynin and taurine (blu circle). Interestingly, two populations are clearly present inside each group: in i) mdx (pink dots) and wt (light blue dots) are almost completely separated indicating that the differences in protein abundance characterize these two different phenotypes; in ii) mdx exe (blue dots) tends to cluster differently from mdx exe treated with compounds (violet and yellow dots) that show the same trend of variation. PCA plot suggests that exercise drastically affect protein pattern and that this effect can be partially modified by taurine and apocynin. In order to identify these spots, preparative 2DE gels were performed and colloidal Coomassie stained. Protein spots are highlighted with circles and numbers in the representative gel shown in Figure 1. These spots were subjected to mass spectrometry analysis and 97 proteins were successfully identified. The results of mass spectrometry identification are reported in Table 1, together with the corresponding spot numbers, ANOVA p-value, adjusted p-value (FDR) and MS data (score and coverage values). The experimental isoelectric point (pI) and molecular mass (Mr) values of the identified proteins mostly matched with those theoretically predicted from the genome sequence although some fragments were present. More than one protein spot was found to correspond to the same protein, consistently with the presence of different post-translationally modified forms of the protein. Trypsin digests of some spots with low Mascot (PMF) score value or with discrepancy between theoretical and calculated MW or pI were further analysed performing peptide sequencing by tandem mass spectrometry. MS/MS analysis was carried out by using an Ultraflex III MALDI-TOF/TOF mass spectrometer (Bruker Daltonics) and the results were reported Table 1 in ref. [27].

PCA analysis pointed out a significant impact of exercise on protein profile of mdx mice: in fact, exercised mdx mice clustered separately from both mdx and wt mice that tend to be closer in PCA biplot. Hence, we dedicated a brief paragraph to the analysis of mdx *vs* wt variations. In fact, differences between wild-type and mdx muscles, at proteomic level, have been widely documented [9-12,28,29], but not in tibialis anterior muscle. Then, we mainly focused our analysis on mdx exe *vs* mdx. The results concerning the effect of taurine and apocynin are reported in a separate paragraph and they were discussed in the light of the main outcomes arising from the comparison between mdx and mdx exe. In Figure 1 and 2 in ref. [27], histograms and picture representing spot abundance variation between each condition are reported.

3.2 Differential abundances of spots in non-exercised mdx tibialis anterior muscle in comparison to wild type

In our proteomic experimental design, we included wild type mice in order to have a referring phenotype. Differences in protein profile between wild-type and mdx hind limb muscles have been widely documented [10,12,28]. However, to our knowledge, the only proteomic study on tibialis anterior muscle, investigated the age-related change in protein abundance in the mdx genotype, while a comparison with wild type has been not described [7]. Hence, in Table 2, the 23 protein spots (corresponding to 15 different proteins) showing a significant difference between mdx and wt animals are reported. The identified proteins mostly belong to sarcomere structure, glucose metabolism and energy transfer. Mdx mice show a down regulation of glycolytic enzymes, Ckm enzyme and a general decrease of sarcomeric proteins. Tibialis anterior muscle is composed mostly by fast glycolytic fibers with high expression of glycolytic enzymes and Ckm in order to support anaerobic metabolism [30]. The general decrease of these enzymes is in agreement with the increased basal expression of slow-genes observed in our study at transcriptional level [15,19] while the decrease in Ckm can be related to the typical loss of the enzyme due to membrane leakiness. Comparable results on protein level, were obtained by D. Gardan-Salmon in gastrocnemius muscle from six weeks old mice [12]. Differently the proteomic analysis performed on three months old

mice (muscles: soleus, extensor digitorum longus, flexor digitorum brevis and interosseous) by Carberry et al. indicated a general increase of both proteins categories with the exceptions of Fructose-bisphosphate aldolase in flexor digitorum brevis and Ckm in soleus [10]. Overall, these data confirm that, muscle types and different ages of mdx mice, must be carefully considered before drawing a general conclusion on the impact of dystrophin lack on muscle protein level.

3.3 Exercise induced protein abundance variation in mdx mice

In mdx mice, exercise induces variation of 64 spots corresponding to 34 different proteins. These spots are indicated in Table 3 together with fold change and Tukey post –ANOVA p-value. To better understand the biological meaning behind the list of identified proteins, we performed a gene ontology (GO) overrepresentation analysis, using the web accessible tool WebGestalt, as specified in Materials and Methods. The enriched GO terms, together with enriched pathways are reported in Figure 3. The most representative information came to light from the enrichment analysis, investigated combining proteomic results with immunoblot approach, are described separately as follows.

Muscle contraction and sarcomere organization

Considering proteins involved in muscle contraction and in sarcomere organization, exercise induces an increase of fast Troponin T (Tnnt3), Troponin I (Tnnt2), Myozenin-1 (Myoz1), Actin and LIM domain-binding protein 3 (Ldb3), whereas Myosin regulatory light chain 2 (Mylpf), Myosin light chain 1/3 (Myl1) and Tropomyosin alpha-1 chain (Tpm1) were downregulated (Figure 4). Interestingly, Tnnt2, Tnnt3 and Myozenin1 are typical fast twitch proteins, and Myoz1 KO induced a fast to slow transition and a decrease in fatigue [31,32]. Then their upregulation is again a sensor of defective adaptation to exercise (in line with gene-expression data) and may in part account for increased fatigability. Mylpf and Myl1 are the two low molecular weight proteins non-covalently attached to myosin molecule. Myosin is a hexameric ATPase cellular motor protein. It is composed of two heavy chains, two non-phosphorylatable alkali light chains, and two

phosphorylatable regulatory light chains. Myl1 is the myosin alkali (or essential) light chain expressed in fast skeletal muscle while Mylpf represents the regulatory and phosphorylatable component. Phosphorylation of Mylpf light chains protein plays a pivotal role in muscle and modulates mechanical aspects of muscle function, resulting in potentiation of isometric and concentric force and in enhancing dynamic aspects of muscle work and power in unfatigued or fatigued muscle [33]. Furthermore, also the abundance of this protein is important since it was demonstrated that extraction of the myosin regulatory light chain 2, disorders myosin head structure, moving them away from the backbone of the thick filament [34]. Its decreasing level, together with the decreasing abundance of Tropomyosin can contribute to explain the reduction of in vivo performance showed by the exercised mice [15]. On the other hand, other important component of sarcomere structure, belonging to thin filaments (Actin, Tnnt3 and Tnnt2) and Z-disk (Ldb3 and Myoz1), resulted up-regulated. Hence, exercise seems to modulate differently the level of the sarcomeres' proteins which may in part account for compensatory mechanisms on function [19]. It is also noteworthy that the three spots corresponding to Lim binding domain protein, that may function as an adapter to couple protein kinase C-mediated signalling via its LIM domains to the cytoskeleton, were increased, but they corresponded to a fragment of the protein. In fact, checking the apparent molecular weight and the peptide coverage, we observed that these spots have an apparent molecular weight lower than the one expected and furthermore, the peptide coverage is limited to the N-terminus of the protein, suggesting an activation of proteolysis (Table 2 in ref. [27]). It is also interesting to note an increased level of two spots, corresponding to Tnnt3, which showed a shift in pI value, indicating that exercise increased the level of a Tnn3 isoform harbouring post-translational modification. The variation of actin abundance was confirmed by immunoblot analysis shown in Figure 5A.

In Table 3 in ref [27] we also reported the differentially abundant proteins between mdx exe and wt. It is worth noting that in mdx exercised mice, the number of proteins that show a different level in

comparison to wt is greater than in the comparison mdx vs wt (34 and 22 respectively). In particular, concerning sarcomere protein abundance, we found that exercise induce a further decrease of proteins directly involved in contraction (Tpm1, Tpm2, Actin and Mylpf) whereas proteins belonging to Z-disk (Ldb3, Myot) resulted increased.

Glycolysis and gluconeogenesis pathways

Glucose metabolism results greatly modified in mdx mice after exercise. In fact, we found several spots corresponding to three enzymes of glycolysis, Fructose-bisphosphate aldolase A, Triosephosphate isomerase, Beta-enolase (Aldoa, Tpi1, Eno3), with an increased level after exercise. We also include in this group the enzyme UTP-glucose-1-phosphate uridylyltransferase (Ugp2) that has a central role as a glucosyl donor in glycogen synthesis and in the production of glycolipids, glycoproteins, and proteoglycans. This enzyme resulted also up regulated after exercise. In order to validate the proteomic results, we performed an immunoblot of AldoA, EnoB and Tpi1 enzymes (Figure 5 B).

TCA cycle and respiratory chain complex

After exercise, two enzymes of TCA cycle resulted increased: Fumarate hydratase (Fh) and Malate dehydrogenase (Mdh2). These two enzymes are involved in the two final steps of oxaloacetate regeneration that can be used for both TCA cycle and amino acids production. We included in this group also the enzyme Delta-1-pyrroline-5-carboxylate dehydrogenase (Aldh4a1) that catalyses the irreversible conversion of delta-1-pyrroline-5-carboxylate derived from either proline or ornithine, to glutamate and plays an important role in suppling intermediate substrates of TCA; also, this enzyme is up-regulated after exercise. Concerning electron transport chain and ATP production, we found a decreased abundance of NADH dehydrogenase [ubiquinone] 1 beta subcomplex subunit 7 (Ndufb7), a protein that belongs to Complex I and an increased level of a fragment of ATP synthase subunit alpha (Atp5a1) that belongs to the catalytic core of ATP synthase. To better analyse the abundance of electron chain complexes and to bring out differences in the amount of low abundant

proteins that could not be easily detected in a total protein extract by 2DE, we performed an immunoblot using Total OXPHOS Rodent WB Antibody Cocktail. This cocktail contains 5 mouse mAbs, against one subunit of each complex (Figure 6). By immunoblot we confirmed the decreased concentration of complex I and we uncovered an increased level of complex II and a decreased level of complex III, whereas complex IV and complex V resulted unchanged. As shown in Figure 7, exercise induces a general increase of enzymes involved in glucose metabolism and in TCA cycle, whereas, concerning electron transport chain and ATP production, complex I and III showed a reduced abundance while complex II had the opposite behaviour. This could be explained considering that complex II is strictly connected to TCA cycle. In fact, the succinate dehydrogenase belongs to complex II, thus the oxidation of succinate to fumarate is the sole Krebs reaction that takes place on the inner membrane itself, as opposed to the other reactions that are catalysed by soluble enzymes [35]. The energy carrier flavin adenine dinucleotide (FAD) is also a part of the succinate dehydrogenase complex. Hence, the increased level of this complex is in agreement with the increased level of TCA enzymes. It is also important to underline that also in severely compromised mitochondria, succinate dehydrogenase activity, can usually be spared, as long as fragments of the inner membrane remain [36]. In this context, we can speculate that in exercised mdx mice, there is an increased level of anaerobic metabolism (increased glycolysis), while mitochondria function could be partially compromised. In this scenario, the role of TCA cycle could be the anaplerotic one: it means that the cycle could be mostly used to produce precursors of other metabolic compounds. In fact, we found an up-regulation of Aldh4a1, involved in the synthesis of glutamate from alpha-ketoglutarate and up-regulation of Fh, and Mdh2 involved regeneration of oxaloacetate that can be used for amino acid synthesis.

Energy transfer

Creatine kinase (Ckm) and Adenylate kinase (Ak1) are essential enzymes in tissues characterized by high and sudden increases of energy demand. After exercise, we observed an increased level of

several spots of Ckm whereas Ak1 shows a marked decrease when compared with mdx. Ak1 catalysed the reversible reaction ATP+AMP to 2ADP and it represents the key enzymes in the synthesis and equilibration of adenine nucleoside [37]. A reduction of Ak1 expression in mdx mice in comparison to wild-type, was detected by Ge Y. et al in mdx hindlimb muscles. [11] These authors also demonstrated that the decline of active Ak1 activity correlated with increased Ckm activity, suggesting that a compensatory energy metabolism mechanism might exist in mdx mouse skeletal muscle. Furthermore, it was observed that, in Ak1 knockout mice, there is a deep alteration of energetic homeostasis. In fact, in these mice, the nucleotide levels are maintained, but the glycolytic flux and Ckm-P turnover are increased [38]. Our results clearly indicate that exercise induce a decrease of Ak1 protein level and an increased level of glycolytic enzymes (Eno3, Aldoa, Tpis1). These findings suggest that in exercised mdx mice, as showed for Ak1 knockout mice, there is a compensatory increase of glycolytic pathway. According to this observation, in mdx exe, we also found an increased level of several spots of Ckm. Concerning this enzyme, it must be highlighted that several spots (55, 56, 57, 58, 59, 60) presented an experimental molecular weight lower than the one expected (Table 1) indicating that the increased level of this protein (observed for spots 61, 62,64, 65, 67 and 69), is also combined with and increased proteolysis. The protein peptide coverage of these spots, Table 2 of ref [27], indicates that they correspond to amino-terminal fragment of the protein.

3.4 Exercise related proteins

PGC1-alpha and its upstream regulator Sirt1 are key proteins involved in muscle response to exercise [39]. In particular, PGC1-alpha is an important regulator of mitochondrial bio-genesis and oxidative metabolism and it is involved in fast to slow transition of muscle fibres. Sirt1 is induced by NAD^+ and regulates metabolism by repressing glycolytic genes [40,41]. In a previous study we demonstrated that PGC1-alpha and its upstream regulator Sirt1 genes were up-regulated in mdx versus age-matched wt muscles in basal condition and accordingly, an overexpression of signalling

genes related to slow-phenotype genes was evident [15]. Furthermore, we demonstrated that, PGC1-alpha and Sirt1 genes expression remained stable after 4 weeks of exercise and decrease after a more prolonged exercise protocol (16 weeks). This trend is opposite of the one observed in wild type mice subjected to exercise [42] and clearly indicates a maladaptation to exercise of mdx mice. In order to confirm these data also at protein level, we performed an immunoblot of PGC1-alpha and Sirt1. We include in this blot also the wild-type mice, since the increased protein level of these two proteins in non-exercised mdx is important to better understand the mdx muscle response to exercise. As shown in Figure 8, immunoblot confirmed the data obtained with our previous gene expression analysis, indicating that both proteins are more expressed abundant in mdx mice in comparison to control mice. After exercise, the protein level of PGC1-alpha and Sirt1 were unchanged, unless a tendency to decrease was detected for Sirt1.

3.5 Apocynin and taurine modulation of proteomic changes induced by exercise

In a previous study we showed the ability of apocynin and taurine in counteracting some of the deleterious effects induced by the exercise [16]. Here, the effects of these compounds were analysed at a proteomic level. As shown in the PCA biplot (Figure 2), exercise was the main source of variation between the groups analysed in this study, but the treatment with taurine and apocynin represented a partially separated clusters of protein abundance modification. We divided these protein spots in three groups presented in Table 4. The first group is formed by proteins whose level is modified by exercise, but that, with taurine and/or apocynin treatment, show a reduction of this modification that became non-significant. The second group includes spots that show a significant variation between mdx exe and mdx exe treated with compounds. Most of the proteins of these two groups, belonged to glucose metabolism and energy transfer pathways, both resulted increased after exercise. The data related to these two groups, mean that these treatments were able to counteract the effect that exercise induced on the abundance of these proteins and that in some cases, (group II) this effect is significantly reverted. It is interesting to note that proteins involved in sarcomere

organization or muscle contraction were little represented in this two groups (spot 2 corresponding to Ldb3, spot 18 corresponding to Tpm1 and spot 22 corresponding to Actin). Lastly, the third group is composed by spots that behave in intermediate way between the two previous groups. In this group, we found two spots corresponding to Troponin T and Troponin I whose increase abundance induced by exercise, is reduced by apocynin treatment. See also Figure 1 in ref. [27] for a detailed report of spot variations. All the spots not present in these three groups showed the same behaviour after exercise. (i.e. they were significantly modified with or without treatments). In Figure 9 a clustering representation the three groups is reported.

4. Conclusions

The exercised mdx mice present a more severe phenotype than sedentary mdx, in fact they show an increased weakness and fatigability, along with muscle necrosis and fibrosis, elevated oxidative stress and worsened calcium homeostasis [43,44]. However, the molecular mechanisms responsible for the intolerance to exercise are not fully understood. In a previous work, based on gene expression profiling of key proteins involved in exercise response, we showed that dystrophic muscles have a defect in mechano-transduction signalling and that this defect is mostly ascribable to Sirt1, PGC1-alpha related pathways. In fact, we showed that Sirt1 and PGC1-alpha RNAs are higher in mdx animal than in wt and that exercise induces a significant and marked reduction in PGC1-alpha expression, particularly evident after 16 weeks of exercise [15]. In this study, we analysed, for the first time, the impact of a chronic exercise protocol, on protein abundance in tibialis anterior muscle of mdx mice. Our data, together with previously data performed on RNA level, indicate that mdx mice show a higher basal level of PGC1-alpha and Sirt1 proteins in comparison to wt. In agreement with gene expression data in GC muscle, four weeks of exercise are not able to induce variation in protein abundance of these two proteins but clearly failed to stimulate the metabolic changes associated to fast-to-slow transition typically observed in aerobically trained muscle [45,46]. In fact, mdx exercised mice display an increased level of several enzymes of

glycolysis, Krebs cycle and related anaplerotic pathways whereas complex I and Complex III of the electron transport chain are decreased. It also worth noting the strong down regulation of Ak1 enzyme in mdx exercised mice. In healthy muscles expression of adenylate kinase isoforms increases in response to exercise [47]. In fact, the catalytic function of adenylate kinase is particularly important in tissues with high and fluctuating energy demands since it allows the utilization of the second high-energy bond of the β-phosphoryl in the ATP molecule, thereby doubling the energetic potential that the cell can use. Furthermore, by sensing the energy status of muscle cells and regulating gene expression, the Ak1 and downstream AMP signalling are critical regulators of mitochondrial biogenesis, through the AMPK-PGC-alpha signalling cascade [48]. Importantly, we recently showed that a long exercise protocol led to a significant increase of pAMPK/AMPK in wt muscles, while it failed to adapt the higher pAMPK/AMPK ratio observed in sedentary mdx muscles [19]. Hence, why Ak1 is downregulated by exercise, and how this downregulation is related to a compensatory rearrangement of energy production and eventually to an alteration of AMP mediated signalling, are important points that need to be more investigated. However, at the moment, this represents an important mechanism for altered mechanical-metabolic coupling in dystrophic muscle. Concerning proteins involved in muscle structure and contraction, it is interesting to note that sedentary mdx mice show a downregulation of Mylpf, Tpm2 and Tpm1 and that this trend is worsened by exercise and this is particularly evident for Mylpf. On the other hand, in exercised mdx some proteins of Z-disk and of thin filaments are upregulated in comparison to non-exercised mdx, although some of them correspond to a fragment of the protein. Taken together these results confirm the global alteration of the abundance of sarcomeres' proteins and suggest that exercise could exacerbate this feature both decreasing the expression of myosin regulatory light chain 2 and/or enhancing specific protein degradation. Interestingly, the present data confirm the complex mechanism of action of natural anti-oxidant compounds, which may account for the partial benefit observed in degenerative muscle conditions and that can be related to

their ability to dynamically interact with metabolism and endogenous anti-oxidant pathways [16,49].

Fundings

This work has been supported by Dutch Duchenne Parent Project (DPP-NL) 2015 and Italian PRIN n. 2015MJBEM2_005.

Acknowledgements

The authors thank Matteo Ramazzotti from Department of Experimental and Clinical Biomedical Sciences “Mario Serio”, University of Florence, Florence, Italy, for generous assistance with the statistical analysis.

References

[1] G. Bulfield, W.G. Siller, P.A. Wight, K.J. Moore, X chromosome-linked muscular dystrophy (mdx) in the mouse., Proc. Natl. Acad. Sci. U. S. A. 81 (1984) 1189–92. doi:10.1073/pnas.81.4.1189.

[2] T.A. Partridge, The mdx mouse model as a surrogate for Duchenne muscular dystrophy, FEBS J. 280 (2013) 4177–4186. doi:10.1111/febs.12267.

[3] M.D. Grounds, H.G. Radley, G.S. Lynch, K. Nagaraju, A. De Luca, Towards developing standard operating procedures for pre-clinical testing in the mdx mouse model of Duchenne muscular dystrophy, Neurobiol. Dis. 31 (2008) 1–19. doi:10.1016/j.nbd.2008.03.008.

[4] J.K. McGeachie, M.D. Grounds, T.A. Partridge, J.E. Morgan, Age-related changes in replication of myogenic cells in mdx mice: Quantitative autoradiographic studies, J. Neurol. Sci. 119 (1993) 169–179. doi:10.1016/0022-510X(93)90130-Q.

[5] J. Hyzewicz, U.T. Ruegg, S. Takeda, Comparison of Experimental Protocols of Physical Exercise for mdx Mice and Duchenne Muscular Dystrophy Patients., J. Neuromuscul. Dis. 2 (2015) 325–342. doi:10.3233/JND-150106.

[6] C.D. Markert, F. Ambrosio, J.A. Call, R.W. Grange, Exercise and Duchenne muscular dystrophy: Toward evidence-based exercise prescription, Muscle and Nerve. 43 (2011) 464–478. doi:10.1002/mus.21987.

[7] S. Carberry, M. Zweyer, D. Swandulla, K. Ohlendieck, Profiling of age-related changes in the tibialis anterior muscle proteome of the mdx mouse model of dystrophinopathy, J. Biomed. Biotechnol. 2012 (2012). doi:10.1155/2012/691641.

[8] C. Lewis, H. Jockusch, K. Ohlendieck, Proteomic Profiling of the Dystrophin-Deficient MDX Heart Reveals Drastically Altered Levels of Key Metabolic and Contractile Proteins, 2010 (2010). doi:10.1155/2010/648501.

[9] P. Doran, G. Martin, P. Dowling, H. Jockusch, K. Ohlendieck, Proteome analysis of the dystrophin-deficient MDX diaphragm reveals a drastic increase in the heat shock protein cvHSP, Proteomics. 6 (2006) 4610–4621. doi:10.1002/pmic.200600082.

[10] S. Carberry, H. Brinkmeier, Y. Zhang, C.K. Winkler, K. Ohlendieck, Comparative proteomic profiling of soleus, extensor digitorum longus, flexor digitorum brevis and interosseus muscles from the mdx mouse model of Duchenne muscular dystrophy, Int. J. Mol. Med. 32 (2013) 544–556. doi:10.3892/ijmm.2013.1429.

[11] Y. Ge, M.P. Molloy, J.S. Chamberlain, P.C. Andrews, Proteomic analysis of mdx skeletal muscle: Great reduction of adenylate kinase 1 expression and enzymatic activity, Proteomics. 3 (2003) 1895–1903. doi:10.1002/pmic.200300561.

[12] D. Gardan-Salmon, J.M. Dixon, S.M. Lonergan, J.T. Selsby, Proteomic assessment of the acute phase of dystrophin deficiency in mdx mice, Eur. J. Appl. Physiol. 111 (2011) 2763–2773. doi:10.1007/s00421-011-1906-3.

[13] S. Fontana, O. Schillaci, M. Frinchi, M. Giallombardo, G. Morici, V. Di Liberto, et al., Reduction of mdx mouse muscle degeneration by low-intensity endurance exercise: a proteomic analysis in quadriceps muscle of exercised versus sedentary mdx mice, Biosci. Rep. (2015) 1–10. doi:10.1042/BSR20150013.

[14] J. Hyzewicz, J. Tanihata, M. Kuraoka, N. Ito, Y. Miyagoe-Suzuki, S. Takeda, Low intensity training of mdx mice reduces carbonylation and increases expression levels of proteins involved in energy metabolism and muscle contraction, Free Radic. Biol. Med. 82 (2015) 122–136. doi: 10.1016/j.freeradbiomed.2015.01.023.

[15] G.M. Camerino, M. Cannone, A. Giustino, A.M. Massari, R.F. Capogrosso, A. Cozzoli, et al., Gene expression in mdx mouse muscle in relation to age and exercise: aberrant mechanical-metabolic coupling and implications for pre-clinical studies in Duchenne muscular dystrophy., Hum. Mol. Genet. 39 (2014) 1–13. doi:10.1093/hmg/ddu287.

[16] R.F. Capogrosso, A. Cozzoli, P. Mantuano, G.M. Camerino, A.M. Massari, V.T. Sblendorio, et al., Assessment of resveratrol, apocynin and taurine on mechanical-metabolic uncoupling and oxidative stress in a mouse model of duchenne muscular dystrophy: A comparison with the gold standard, α-methyl prednisolone, Pharmacol. Res. 106 (2016) 101–113. doi: 10.1016/j.phrs.2016.02.016.

[17] S. Pierno, B. Nico, R. Burdi, A. Liantonio, M.P. Didonna, V. Cippone, et al., Role of tumour necrosis factor alpha, but not of cyclo-oxygenase-2- derived eicosanoids, on functional and morphological indices of dystrophic progression in mdx mice: A pharmacological approach, Neuropathol. Appl. Neurobiol. 33 (2007) 344–359. doi:10.1111/j.1365-2990.2007.00798. x.

[18] A. De Luca, B. Nico, A. Liantonio, M.P. Didonna, B. Fraysse, S. Pierno, et al., A Multidisciplinary Evaluation of the Effectiveness of Cyclosporine A in Dystrophic Mdx Mice, (2005). doi:10.1016/S0002-9440(10)62270-5.

[19] R.F. Capogrosso, P. Mantuano, A. Cozzoli, F. Sanarica, A.M. Massari, E. Conte, et al., Contractile efficiency of dystrophic mdx mouse muscle: in vivo and ex vivo assessment of adaptation to exercise of functional end points, J. Appl. Physiol. 122 (2017) 828–843. doi:10.1152/japplphysiol.00776.2015.

[20] F. Magherini, P.M. Abruzzo, M. Puglia, L. Bini, T. Gamberi, F. Esposito, et al., Proteomic analysis and protein carbonylation profile in trained and untrained rat muscles, J. Proteomics. 75 (2012) 978–992. doi: 10.1016/j.jprot.2011.10.017.

[21] D. Wessel, U.I. Flügge, A method for the quantitative recovery of protein in dilute solution in the presence of detergents and lipids, Anal. Biochem. 138 (1984) 141–143. doi:10.1016/0003-2697(84)90782-6.

[22] D.F. Hochstrasser, A. Patchornik, C.R. Merril, Development of polyacrylamide gels that improve the separation of proteins and their detection by silver staining, Anal. Biochem. 173 (1988) 412–423. doi:10.1016/0003-2697(88)90208-4.

[23] V. Neuhoff, N. Arold, D. Taube, W. Ehrhardt, Improved staining of proteins in polyacrylamide gels including isoelectric focusing gels with clear background at nanogram sensitivity using Coomassie Brilliant Blue G-250 and R-250, Electrophoresis. 9 (1988) 255–262. doi:10.1002/elps.1150090603.

[24] N.A. Karp, M. Spencer, H. Lindsay, K. O'Dell, K.S. Lilley, Impact of replicate types on proteomic expression analysis, J. Proteome Res. 4 (2005) 1867–1871. doi:10.1021/pr050084g.

[25] B. Zhang, S. Kirov, J. Snoddy, WebGestalt: An integrated system for exploring gene sets in various biological contexts, Nucleic Acids Res. 33 (2005) 741–748. doi:10.1093/nar/gki475.

[26] E.K. Schneider CA, Rasband WS, NIH Image to ImageJ: 25 years of image analysis., Nat. Methods. 9 (2012) 671–675.

[27] T. Gamberi, T. Fiaschi, E. Valocchia, A. Modesti, P. Mantuano, J.F. Rolland, F. Sanarica, A. De Luca and Francesca Magherini, Protein abundance alteration induced by chronic exercise in mdx mice model of Duchenne muscular dystrophy and potential modulation by apocynin and taurine. Data in Brief, submitted.

[28] S. Rayavarapu, W. Coley, E. Cakir, V. Jahnke, S. Takeda, Y. Aoki, et al., Identification of disease specific pathways using in vivo SILAC proteomics in dystrophin deficient mdx mouse., Mol. Cell. Proteomics. 12 (2013) 1061–73. doi:10.1074/mcp.M112.023127.

[29] C. Lewis, S. Carberry, K. Ohlendieck, Proteomic profiling of x-linked muscular dystrophy, J. Muscle Res. Cell Motil. 30 (2009) 267–279. doi:10.1007/s10974-009-9197-6.

[30] S. Schiaffino, C. Reggiani, Fiber types in mammalian skeletal muscles., Physiol. Rev. 91 (2011) 1447–531. doi:10.1152/physrev.00031.2010.

[31] N. Frey, D. Frank, S. Lippl, C. Kuhn, H. Kögler, T. Barrientos, et al., Calsarcin-2 deficiency increases exercise capacity in mice through calcineurin / NFAT activation, 118 (2008). doi:10.1172/JCI36277.3598.

[32] Z.-B. Yu, F. Gao, H.-Z. Feng, J.-P. Jin, Differential regulation of myofilament protein isoforms underlying the contractility changes in skeletal muscle unloading, (n.d.). https://www.ncbi.nlm.nih.gov/pmc/articles/PMC1820608/pdf/nihms14160.pdf (accessed April 19, 2017).

[33] K.E. Kamm, J.T. Stull, Signaling to myosin regulatory light chain in sarcomeres, J. Biol. Chem. 286 (2011) 9941–9947. doi:10.1074/jbc. R110.198697.

[34] R.J. Levine, Z. Yang, N.D. Epstein, L. Fananapazir, J.T. Stull, H.L. Sweeney, Structural and functional responses of mammalian thick filaments to alterations in myosin regulatory light chains., J. Struct. Biol. 122 (1998) 149–61. doi:10.1006/jsbi.1998.3980.

[35] A. Peeters, A.B. Shinde, R. Dirkx, J. Smet, K. De Bock, M. Espeel, et al., Mitochondria in peroxisome-deficient hepatocytes exhibit impaired respiration, depleted DNA, and PGC-1α independent proliferation, Biochim. Biophys. Acta - Mol. Cell Res. 1853 (2015) 285–298. doi: 10.1016/j.bbamcr.2014.11.017.

[36] H. Schägger, K. Pfeiffer, Supercomplexes in the respiratory chains of yeast and mammalian mitochondria., EMBO J. 19 (2000) 1777–1783. doi:10.1093/emboj/19.8.1777.

[37] P. Dzeja, A. Terzic, Adenylate kinase and AMP signaling networks: metabolic monitoring, signal communication and body energy sensing, Int. J. Mol. Sci. 10 (2009) 1729–1772. doi:10.3390/ijms10041729.

[38] E. Janssen, P.P. Dzeja, F. Oerlemans, a W. Simonetti, a Heerschap, a de Haan, et al., Adenylate kinase 1 gene deletion disrupts muscle energetic economy despite metabolic rearrangement., EMBO J. 19 (2000) 6371–6381. doi:10.1093/emboj/19.23.6371.

[39] C. Handschin, B.M. Spiegelman, The role of exercise and PGC1alpha in inflammation and chronic disease., Nature. 454 (2008) 463–469. doi:10.1038/nature07206.

[40] J.T. Rodgers, C. Lerin, W. Haas, S.P. Gygi, B.M. Spiegelman, P. Puigserver, Nutrient control of glucose homeostasis through a complex of PGC-1a and SIRT1, Nature. 434 (2005) 113–118. doi:10.1038/nature03314.1.

[41] Z. Gerhart-Hines, J.T. Rodgers, O. Bare, C. Lerin, S.-H. Kim, R. Mostoslavsky, et al., Metabolic control of muscle mitochondrial function and fatty acid oxidation through SIRT1/PGC-1α, EMBO J. 26 (2007) 1913–1923. doi:10.1038/sj.emboj.7601633.

[42] C. Handschin, Regulation of skeletal muscle cell plasticity by the peroxisome proliferator-activated receptor gamma coactivator 1alpha, (n.d.). http://edoc.unibas.ch/ (accessed April 14, 2017).

[43] R. Burdi, J.-F. Rolland, B. Fraysse, K. Litvinova, A. Cozzoli, V. Giannuzzi, et al., Multiple pathological events in exercised dystrophic mdx mice are targeted by pentoxifylline: outcome of a large array of in vivo and ex vivo tests, J Appl Physiol. 106 (2009) 1311–1324. doi:10.1152/japplphysiol.90985.2008.

[44] B. Fraysse, A. Liantonio, M. Cetrone, R. Burdi, S. Pierno, A. Frigeri, et al., The alteration of calcium homeostasis in adult dystrophic mdx muscle fibers is worsened by a chronic exercise in vivo, Neurobiol. Dis. 17 (2004) 144–154. doi: 10.1016/j.nbd.2004.06.002.

[45] E. Ferraro, A.M. Giammarioli, S. Chiandotto, I. Spoletini, G. Rosano, Exercise-Induced Skeletal Muscle Remodeling and Metabolic Adaptation: Redox Signaling and Role of Autophagy, Antioxid. Redox Signal. 21 (2014) 154–176. doi:10.1089/ars.2013.5773.

[46] R. Bassel-Duby, E.N. Olson, Signaling pathways in skeletal muscle remodeling., Annu. Rev. Biochem. 75 (2006) 19–37. doi: 10.1146/annurev.biochem.75.103004.142622.

[47] M. Linossier, D. Dormois, C. Perier, J. Frey, A. Geyssant, C. Denis, Enzyme adaptations of human skeletal muscle during bicycle short-sprint training and detraining, Acta Physiol. Scand. 161 (1997) 439–445. doi:10.1046/j.1365-201X.1997.00244. x.

[48] P. Dzeja, A. Terzic, Adenylate Kinase and AMP Signaling Networks: Metabolic Monitoring, Signal Communication and Body Energy Sensing, Int. J. Mol. Sci. Int. J. Mol. Sci. 10 (2009) 1729–1772. doi:10.3390/ijms10041729.

[49] S. Pierno, D. Tricarico, A. Liantonio, A. Mele, C. Digennaro, J.F. Rolland, et al., An olive oil-derived antioxidant mixture ameliorates the age-related decline of skeletal muscle function, Age (Omaha). 36 (2014) 73–88. doi:10.1007/s11357-013-9544-9.

Tables

Table 1 Differentially abundant protein spots, that significantly differed between groups, identified by MALDI TOF mass spectrometry analysis

Spot No[†]	Protein name	AC[‡]	Gene Name	Cellular component Go term	Theoretical	Observed	Mascot search results			ANOVA *p*-value[£]	*FDR* [⊥]
					Mr (kDa)/ pI	Mr (kDa)/ pI [§]	Score[¶]	Matched Pept.[‖]	Seq. coverage (%)[*]		
	Sarcomere organization and muscle contraction										
1	LIM domain-binding protein 3	Q9JKS4	Ldb3	Z-disc	77.6/.7.9	30.1/9.7	86	9/45	17%	0.0135	0.017
2	LIM domain-binding protein 3	Q9JKS4	Ldb3	Z-disc	77.6/.7.9	29.6/9.7	89	11/34	15%	0.0267	0.028
3	LIM domain-binding protein 3	Q9JKS4	Ldb3	Z-disc	77.6/.7.9	30.2/9.3	76	8/34	16%	<0.0001	<0.0001
4	LIM domain-binding protein 3	Q9JKS4	Ldb3	Z-disc	77.6/.7.9	82.4/7	62	7/19	15%	<0.0001	0.0001
5	LIM domain-binding protein 3	Q9JKS4	Ldb3	Z-disc	77.6/.7.9	82.3/6.9	65	9/26	17%	0017	0.0.0043
6	Myozenin-1	Q9JK37	Myoz1	Cytoskeleton	31.4/8.6	31.7/7.9	121	15/77	67%	0.0003	0.0006
7	Troponin I, fast skeletal muscle	P13412	Tnnt2	Troponin complex	21.5/8.6	21.5/8.6	107	12/29	44%	<0.0001	0.0003
8	Troponin I, fast skeletal muscle	P13412	Tnnt2	Troponin complex	21.5/8.6	21.6/8.4	100	12/55	47%	0.021	0.0242
9	Troponin I, fast skeletal muscle	P13412	Tnnt2	Troponin complex	21.5/8.6	21.5/8.5	100	17/58	52%	<0.0001	0.0002
10	Troponin T, fast skeletal muscle	Q9QZ47	Tnnt3	Troponin complex	32.2/5.3	32.9/6.9	70	8/27	31%	0.0062	0.01
11	Troponin T, fast skeletal muscle	Q9QZ47	Tnnt3	Troponin complex	32.2/5.3	31.5/7.8	82	10/43	33%	<0.0001	0.0001
12	Troponin T, fast skeletal muscle	Q9QZ47	Tnnt3	Troponin complex	32.2/5.3	31.9/9.2	74	8/27	26%	0.021	0.022
13	Myosin regulatory light chain 2, skeletal muscle isoform	P97457	Mylpf	Myosin complex	19/4.8	16.1/4.8	88	10/42	63%	0.0066	0.038
14	Myosin regulatory light chain 2, skeletal muscle isoform	P97457	Mylpf	Myosin complex	19/4.8	16.1/4.9	157	17/65	79%	0.0009	0.008
15	Myosin regulatory light chain 2, skeletal muscle isoform	P97457	Mylpf	Myosin complex	19/4.8	17/4.9	132	10/28	63%	<0.0001	<0.0001
16	Myosin regulatory light chain 2, skeletal muscle isoform	P97457	Mylpf	Myosin complex	19/4.8	17.1/4.9	72	6/36	37%	<0.0001	<0.0001
17	Tropomyosin beta chain	P58774	Tpm2	Cytoskeleton	32.9/4.7	36.1/4.9	74	11/38	29%	<0.0001	0.0003
18	Tropomyosin alpha-1 chain	P58771	Tpm1	Cytoskeleton	32.7/4.7	34.3/4.9	109	12/30	32%	<0.0001	0.0014
19	Myosin light chain 1/3, skeletal muscle isoform	P05977	Myl1	Myosin complex	20.7/4.9	21.3/5.2	70	6/33	49%	<0.0001	0.0008
20	Myosin light chain 1/3, skeletal muscle isoform	P05977	Myl1	Myosin complex	20.7/4.9	24.6/5.1	71	8/32	38%	<0.0001	<0.0001
21	Myosin light chain 1/3, skeletal muscle isoform	P05977	Myl1	Myosin complex	20.7/4.9	21.1/5.1	65	5/22	37%	<0.0001	0.028
22	Actin, alpha skeletal muscle and Actin, alpha cardiac muscle1	P68134 and P68033	Acta1 and Actc1	Cytoskeleton	42.3/5.2	51.2/5.1	62	6/18	23%	0.006	0.035
23	Actin, alpha skeletal muscle and Actin, alpha cardiac muscle1	P68134 and	Acta1 and Actc1	Cytoskeleton	42.3/5.2	42.4/5.2	72	14/32	44%	0.0128	0.034

	Transitional endoplasmic reticulum ATPase (mix)[a]	P68033 Q01853	Vcp	Proteasome complex	89.9/5.1	42.4/5.2	73	8/30	27%		
24	Actin, alpha cardiac muscle 1	P68033	Actc1	Cytoskeleton	42.3/5.2	42.6/5.2	55	5/17	18%	0.0003	0.0013
25	Actin, alpha skeletal muscle	P68134	Acta1	Cytoskeleton	42.3/5.2	42.6/5.1	134	14732	17%	0.0098	0.014
26	Myotilin	Q9JIF9	Myot	Cytoskeleton/sarcolemma	55.7/9.2	59.5/9	64	7/21	16%	0.0072	0.003
27	Myotilin	Q9JIF9	Myot	Cytoskeleton/sarcolemma	55.7/9.2	59.5/9.4	71	7/21	22%	<0.0001	<0.0001
	Metabolism										
	(Glucose metabolism)										
28	Fructose-bisphosphate aldolase A	P05064	Aldoa	cytoplasm	39.7/8.3	38.3/7.4	117	13/47	52%	0.009	0.0135
29	Fructose-bisphosphate aldolase A	P05064	Aldoa	cytoplasm	39.7/8.3	38.1/7.6	135	14/42	60%	0.012	0.0161
30	Fructose-bisphosphate aldolase A	P05064	Aldoa	cytoplasm	39.7/8.3	30.4/7.1	60	6/25	16%	<0.0001	<0.0001
31	Fructose-bisphosphate aldolase A	P05064	Aldoa	cytoplasm	47.3/6.7	31.5/6.8	100	9/28	36%	0.007	0.0115
32	Triosephosphate isomerase	P17751	Tpi1	cytoplasm	32.7/5.5	24.9/6.4	117	11/37	45%	<0.0001	<0.0001
33	Triosephosphate isomerase	P17751	Tpi1	cytoplasm	32.7/5.5	25/6.7	122	12/58	49%	0.006	0.0109
34	Triosephosphate isomerase	P17751	Tpi1	cytoplasm	32.7/5.5	25/6.7	91	8/26	34%	0.004	0.0079
35	Triosephosphate isomerase	P17751	Tpi1	cytoplasm	32.7/5.5	24.3/6.1				0.033	0.0035
36	Triosephosphate isomerase	P17751	Tpi1	cytoplasm	32.7/5.5	24.9/6.5	105	10/39	48%	<0.0001	<0.0001
37	Beta-enolase	P21550	Eno3	cytoplasm	47.3/6.7	46.6/6.3	95	8/22	23%	0.035	0.034
38	Beta-enolase	P21550	Eno3	cytoplasm	47.3/6.7	46.7/6.3	109	12/41	37%	0.012	0.0159
39	Beta-enolase	P21550	Eno3	cytoplasm	47.3/6.7	46.5/6.6	121	15/39	39%	0.005	0.0019
40	Beta-enolase	P21550	Eno3	cytoplasm	47.3/6.7	46.5/6.4	121	12/30	37%	0.017	0.0213
41	UTP--glucose-1-phosphate uridylyltransferase	Q91ZJ5	Ugp2	Cytoplasm and nucleus	57.1/7.2	53.8/6.8	94	9/21	26%	0.0005	0.0017
	(TCA cycle and associate metabolic pathways)										
42	Fumarate hydratase, mitochondrial	P97807	Fh	mitochondrion	54.5/9.1	45.7/7.1	76	12/32	28%	0.001	0.003
43	Fumarate hydratase, mitochondrial	P97807	Fh	mitochondrion	54.5/9.1	45.7/7.5	128	16/46	42%	0.002	0.005
44	Malate dehydrogenase, mitochondrial	P08249	Mdh2	Mitochondrion		35.7/8.2				0.0002	0.0008
45	Dihydrolipoyl dehydrogenase, mitochondrial	O08749	Dld	mitochondrion	54.7/7.9	32.9/8.3	93	11/48	28%	0.002	0.005
46	Delta-1-pyrroline-5-carboxylate dehydrogenase, mitochondrial	Q8CHT0	Aldh4a1	mitochondrion	62.2/8.4	63/6.8	70	8/30	22%	0.013	0.017
47	Aconitate hydratase, mitochondrial	Q99KI0	Aco2	mitochondrion	86.1/8.1	86.1/6.8	96	10/21	26%	0.002	0.005
	(Respiratory chain complex)										
48	NADH dehydrogenase [ubiquinone] flavoprotein 2, mitochondrial	Q9D6J6	Ndufv2	mitochondrion	27.6/7	23.9/5.4	71	8/32	38%	0.002	0.026
49	NADH dehydrogenase [ubiquinone] 1 beta subcomplex subunit 7	Q9CR61	Ndufb7	mitochondrion	16.5/8.3	16.7/8.4	65	5/25	51%	0.009	0.014
50	Cytochrome b-c1 complex subunit 1, mitochondrial	Q9CZ13	Uqcrc1	mitochondrion	53.4/5.8	46.1/5.3	101	11/26	26%	0.009	0.013
51	ATP synthase subunit alpha, mitochondrial	Q03265	Atp5a1	mitochondrion	59.8/9.22	22.5/6.6	72	7/22	17%	0.032	0.033

				(Fatty acid metabolic process)							
52	Fatty acid-binding protein, heart	P11404	Fabp3	Cytoplasm	14.8/6.1	12.4/5.8	82	5%12	40%	0.0013	0.017
53	Enoyl-CoA hydratase, mitochondrial	Q8BH95	Echs1	Mitochondrion	31.8/8.8	26.5/8.0	104	9/25	36%	0.049	0.044
54	Succinyl-CoA:3-ketoacid coenzyme A transferase 1, mitochondrial	Q9D0K2	Oxct1	Mitochondrion	56.3/8.7	55.7/6.9	71	10/35%	29%	0.0002	0.0008
				Energy transfert							
55	Creatine kinase M-type	P07310	Ckm	cytoplasm	43.2/6.6	24.3/6.3	61	7/20	21%	<0.0001	<0.0001
56	Creatine kinase M-type	P07310	Ckm	Cytoplasm	43.2/6.6	28.8/6.6	69	8/25	22%	0.012	0.016
57	Creatine kinase M-type	P07310	Ckm	Cytoplasm	43.2/6.6	29/6.6	66	10/39	27%	<0.0001	<0.0001
58	Creatine kinase M-type	P07310	Ckm	Cytoplasm	43.2/6.6	29.7/6.6	61	7/35	21%	0.0002	0.0008
59	Creatine kinase M-type	P07310	Ckm	Cytoplasm	43.2/6.6	24.4/6.5	64	6/21	18%	0.002	0.005
60	Creatine kinase M-type	P07310	Ckm	Cytoplasm	43.2/6.6	17.4/7.9	68	9/34	29%	0.002	0.005
61	Creatine kinase M-type	P07310	Ckm	Cytoplasm	43.2/6.6	53.3/6.6	89	8/17	26%	0.018	0.023
62	Creatine kinase M-type	P07310	Ckm	Cytoplasm	43.2/6.6	40.4/6.4	88	11/47	32%	<0.0001	<0.0001
63	Creatine kinase M-type	P07310	Ckm	Cytoplasm	43.2/6.6	40.4/6.4	119	13/25	45%	0.0003	0.0013
64	Creatine kinase M-type	P07310	Ckm	Cytoplasm	43.2/6.6	40.7/6.5	133	13/34	46%	0.009	0.014
65	Creatine kinase M-type	P07310	Ckm	Cytoplasm	43.2/6.6	40.2/6.6	177	19/61	51%	0.01	0.015
66	Creatine kinase M-type	P07310	Ckm	Cytoplasm	43.2/6.6	41/7.8	58	7/22	24%	0.014	0.018
67	Creatine kinase M-type	P07310	Ckm	Cytoplasm	43.2/6.6	59.6/6.6	116	8/18	29%	0.015	0.019
68	Creatine kinase S-type, mitochondrial	Q6P8J7	Ckmt2	Mitochondrion	47.9/8.6	41.4/6.1	255	24/57	54%	0.005	0.009
69	Nucleoside diphosphate kinase B	Q01768	Nme2	Nucleus and cytoplasm	17.5/6.9	16.3/6.1	117	10/45	59%	0.0002	0.0009
70	Adenylate kinase isoenzyme 1	Q9R0Y5	Ak1	Cytoplasm	21.6/5.7	21.5/5.3	58	5/20	36%	<0.0001	<0.0001
71	Adenylate kinase isoenzyme 1	Q9R0Y5	Ak1	Cytoplasm	21.6/5.7	22/5.5	104	11/40	55%	0.006	0.009
				Others metabolic process							
72	Alcohol dehydrogenase [NADP(+)]	Q9JII6	Akr1a1	Cytosol	36.8/6.9	26.5/6.6	58	7/46	27%	0.0005	0.002
73	Alcohol dehydrogenase [NADP(+)]	Q9JII6	Akr1a1	Cytosol	36.8/6.9	57/6.1	62	6/20	18%	0.004	0.005
74	Carbonic anhydrase 3	P16015	Ca3	Cytoplasm	29.6/6.9	26.6/7.6	66	5/20	28%	0.002	0.0009
75	Carbonic anhydrase 3	P16015	Ca3	Cytoplasm	29.6/6.9	26.4/6.8	158	12/48	65%	0.0002	0.004
76	Aldehyde dehydrogenase, mitochondrial	P47738	Aldh2	Mitochondrion	57/7.5	51.6/6.27	72	8/26	19%	0.0004	0.001
77	Glyoxylate reductase/hydroxypyruvate reductase	Q91Z53	Grhpr	Cytoplasm	35.7/5.6	35.7/5.57	93	9/30	36%	0.0005	0.002
78	Malate dehydrogenase, cytoplasmic	P14152	Mdh1	Cytoplasm	36.6/6.1	34.2/6.5	68	8/35	25%		
				Transport							
79	Hemoglobin subunit alpha	P01942	Hba	hemoglobin C complex	15.1/7.9	12.3/8.2	90	9/73	66%	0.026	0.028
80	Hemoglobin subunit beta-1	P01942	Hbb-b1	hemoglobin C complex	15.9/7.1	11.9/6.8	111	7/24	56%	0.0002	0.0009
81	Serotransferrin-	Q921I1	Tf	Extracellular region	78.8/6.9	82.6/6.5	106	22%	14/35	<0.0001	<0.0001
82	Serotransferrin	Q921I1	Tf	Extracellular region	78.8/6.9	82.7/6.6	79	20%	10/29	0.001	0.004
83	Serotransferrin	Q921I1	Tf	Extracellular region	78.8/6.9	64.2/6.5	76	17%	9/23	0.011	0.015
84	Serum albumin	P07724	Alb	Extracellular region	70.7/5.6	45.3/6.1	93	21%	11/31	0.031	0.032
85	Serum albumin	P07724	Alb	Extracellular region	70.7/5.6	70.8/5.6	132	33%	17/48	0.014	0.019

86	Serum albumin	P07724	Alb	Extracellular region	70.7/5.6	34.8/5.6	132	33%	17/48	0.0093	0.0137
87	Voltage-dependent anion-selective channel protein 1	Q60932	Vdac1	Mitochondrion	32.5/8.5	29.8/8.6	74	38%	6/21	0.0008	0.002
88	Voltage-dependent anion-selective channel protein 1	Q60932	Vdac1	Mitochondrion	32.5/8.5	29.8/8.2	69	36%	6/22	0.011	0.015
	Others										
89	MICOS complex subunit Mic60	Q8CAQ8	Immt	Mitochondrion	82.2/6.2	73/6.6	75	9/19	16%	0.006	0.01
90	Calpain-7	Q9R1S8	Capn7	Nucleus	93.3/8.1	17.6/10.3	68	10/37	22%	0.025	0.0027
91	26S protease regulatory subunit 8	P62196	Psmc5	Proteasome complex	45.8/7.1	44.6/6.8	78	9/21	26%	0.003	0.006
92	Protein disulfide-isomerase A3	P27773	Pdia3	Endoplasmic reticulum	57.1/5.9	58.9/5.8	73	12/38	26%	0.004	0.007
93	Peroxiredoxin-6	O08709	Prdx6	Cytoplasm	24.9/5.7	24.7/6.2	126	9/24	54%	0.019	0.023
94	Electron transfer flavoprotein subunit alpha, mitochondrial	Q99LC5	Etfa	Mitochondrion	35.5/8.6	34.2/6.6	86	717	30%	0.0007	0.002
95	Heat shock protein beta-1	P14602	Hspb1	Proteasome complex	23/6.1	25.2/6.1	81	8/39	40%	0.013	0.017
96	TBC1 domain family member 5	Q80XQ2	Tbc1d5	Endosome	92.3/6.3	35.1/6.6	57	8/24	14%	0.0005	0.0018
97	Alpha-crystallin B chain	P23927	Cryab	Nucleus	20/6.8	19/6.8	139	11/49	61%	0.013	0.017

†Spot numbers match those reported in the representative 2DE images shown in Figure 1
‡ Accession number in Swiss-Prot/UniprotKB.
§ Based on the calculation using Progenesis SameSpots 4.0 software
¶ MASCOT MS score (Matrix Science, London, UK; http://www.matrixscience.com). MS matching score greater than 56 was required for a significant MS hit (p-value<0.05).
‖ Number of matched peptides correspond to peptide masses matching the top hit from Ms-Fit PMF, searched peptide are also reported.
* Sequence coverage = (number of the identified residues/total number of amino acid residues in the protein sequence) x100%.
£ Anova test was performed by Progenesis SameSpots 4.0 software to determine if the relative change was statistically significant (p<0.05).
⊥ The False Discovery Rate (FDR) was calculated as q-value using Progenesis SameSpots 4.0 software in order to establish how many of the significant ANOVA p-values were false positives. Only the protein spots with an adjusted p-value (FDR)<0.05 were considered for the mass spectrometry analysis.
¤mix Mascot score 105

Table 2. Differentially abundant protein spots between mdx and wt tibialis anterior muscles

Spot No	Protein name	fold change mdx *vs* wt[#]	Tukey post – Anova p-value *
	Sarcomere structure and muscle contraction		
7	Troponin I, fast skeletal muscle	-2.2	0.002
8	Troponin I, fast skeletal muscle	-1.6	0.047
9	Troponin I, fast skeletal muscle	-1.8	<0.0001
16	Myosin regulatory light chain 2, skeletal muscle isoform	-2.1	0.01
17	Tropomyosin beta chain	-2.3	0.0008
18	Tropomyosin alpha-1 chain	-1.8	0.01
23	Actin, alpha skeletal muscle and Actin, alpha cardiac muscle1 Transitional endoplasmic reticulum ATPase	-1.4	0.045
24	Actin, alpha cardiac muscle 1	-1.4	0.021
	Metabolism and energy transfer		
32	Triosephosphate isomerase	-1.53	0.003
33	Triosephosphate isomerase	-1.4	0.031
36	Triosephosphate isomerase	-1.52	0.047
39	Beta-enolase	-1.4	0.011
44	Malate dehydrogenase, mitochondrial	-1.8	0.005
49	NADH dehydrogenase [ubiquinone] 1 beta subcomplex subunit 7	1.8	0.005
50	Cytochrome b-c1 complex subunit 1, mitochondrial	-1.6	0.0036
55	Creatine kinase M-type	-2	0.02
57	Creatine kinase M-type	-2.5	0.0085
59	Creatine kinase M-type	1.8	0.0006
68	Creatine kinase M-type	-1.5	0.029
	Others		
78	Malate dehydrogenase, cytoplasmic	1.4	0.039
81	Serotransferrin	1.5	0.015
93	Peroxiredoxin-6	-1.6	0.019

[#] Fold change (mdx *vs* wt) was calculated dividing the average of %V of mdx by the average of %V of wt (V =volume=integration of the optical density over the spot area; %V = V single spot/V total spots included in the reference gel).
* Tukey's multiple comparisons test was calculated with GraphPad Prism v6.0

Table 3. Differentially abundant protein spots between mdx exe and mdx tibialis anterior muscles

Spot No	Protein name	Fold change mdx exe *vs* mdx[#]	Tukey post – Anova p-value *
	Striated muscle contraction and sarcomere organization		
1	LIM domain-binding protein 3 (Ldb3)	1.52	0.038
2	LIM domain-binding protein 3 (Ldb3)	1.82	0.045
3	LIM domain-binding protein 3 (Ldb3)	1.89	<0.0001
4	LIM domain-binding protein 3 (Ldb3)	1.28	0.018
6	Myozenin-1	1.96	0.002
7	Troponin I, fast skeletal muscle	1.88	0.034
9	Troponin I, fast skeletal muscle	1.58	0.012
11	Troponin T, fast skeletal muscle	2.04	0.002
12	Troponin T, fast skeletal muscle	1.7	0.018
14	Myosin regulatory light chain 2, skeletal muscle isoform	-1.83	0.026
15	Myosin regulatory light chain 2, skeletal muscle isoform	-2.51	0.01
18	Tropomyosin alpha-1 chain	-1.75	0.02
20	Myosin light chain 1/3, skeletal muscle isoform	-2.1	0.002
22	Actin, alpha skeletal muscle and Actin, alpha cardiac muscle1	1.87	0.047
	Glycolysis and gluconeogenesis		
28	Fructose-bisphosphate aldolase A	1.46	0.007
29	Fructose-bisphosphate aldolase A	1.5	0.038
30	Fructose-bisphosphate aldolase A	1.37	0.01
31	Fructose-bisphosphate aldolase A	1.69	0.023
32	Triosephosphate isomerase	1.56	0.002
33	Triosephosphate isomerase	1.45	0.025
34	Triosephosphate isomerase	2.1	0.002
37	Beta-enolase	1.6	0.007
38	Beta-enolase	1.61	0.005
39	Beta-enolase	1.52	0.006
40	Beta-enolase	1.47	0.02
41	UTP--glucose-1-phosphate uridylyltransferase	1.56	<0.0001
	TCA and associated metabolic pathways		
42	Fumarate hydratase, mitochondrial	1.76	0.0009
43	Fumarate hydratase, mitochondrial	1.56	0.0036
44	Malate dehydrogenase, mitochondrial	1.73	0.019
45	Dihydrolipoyl dehydrogenase, mitochondrial	1.38	0.005
46	Delta-1-pyrroline-5-carboxylate dehydrogenase, mitochondrial	1.4	0.005
	Respiratory chain complex		
49	NADH dehydrogenase [ubiquinone] 1 beta subcomplex subunit 7	-1.35	0.025
51	ATP synthase subunit alpha, mitochondrial	1.7	0.03
	Fatty acid metabolic process		
52	Fatty acid-binding protein, heart	-2.3	0.005
53	Enoyl-CoA hydratase, mitochondrial	1.46	0.037
54	Succinyl-CoA:3-ketoacid coenzyme A transferase 1, mitochondrial	1.5	0.005
	Energy transfer		
55	Creatine kinase M-type	2.4	0.0015
56	Creatine kinase M-type	1.9	0.0072
57	Creatine kinase M-type	1.5	0.0041
58	Creatine kinase M-type	2.1	0.028
59	Creatine kinase M-type	-1.9	0.0006
60	Creatine kinase M-type	2.4	0.003
61	Creatine kinase M-type	1.7	0.025
62	Creatine kinase M-type	1.5	0.0019
63	Creatine kinase M-type	1.6	0.018
64	Creatine kinase M-type	1.5	0.008

66	Creatine kinase M-type	2.33	0.032
67	Creatine kinase M-type	1.3	0.013
68	Creatine kinase S-type, mitochondrial	1.5	0.012
69	Nucleoside diphosphate kinase B	5.5	0.003
70	Adenylate kinase isoenzyme 1	-1.9	0.021
	Others		
72	Alcohol dehydrogenase [NADP(+)]	1.7	0.005
74	Carbonic anhydrase 3	1.6	0.007
75	Carbonic anhydrase 3	1.5	0.001
77	Glyoxylate reductase/hydroxypyruvate reductase	1.9	0.002
78	Malate dehydrogenase, cytoplasmic	-1.3	0.005
	Transport		
82	Serotransferrin	1.5	0.028
84	Serum albumin	1.87	0.047
86	Serum albumin	-1.3	0.0006
87	Voltage-dependent anion-selective channel protein 1	1.4	0.007
88	Voltage-dependent anion-selective channel protein 1	1.4	0.008
89	MICOS complex subunit Mic60	1.3	0.032
91	26S protease regulatory subunit 8	1.5	0.021
94	Electron transfer flavoprotein subunit alpha, mitochondrial	1.6	0.014

[#] Fold change (mdx exe vs mdx) was calculated dividing the average of %V of mdx exe by the average of %V of mdx (V =volume=integration of the optical density over the spot area; %V = V single spot/V total spots included in the reference gel).
* Tukey's multiple comparisons test was calculated with GraphPad Prism.

Table 4. Groups of proteins whose abundance was differently modified by the combination of exercise with apocynin or taurine treatment.

		Comparison *vs* mdx[¤]			Comparison *vs* mdx[¤] exe	
Spot No	**Protein name**	**exercise** [*]	**apocynin**[†]	**taurine**[†]	**apocynin**[≠]	**taurine**[≠]
		Group I				
2	LIM domain-binding protein 3	**1.52**	*ns (1.6)*	*ns (1.6)*	*ns (-1.2)*	*ns (-1.1)*
18	Tropomyosin alpha-1 chain	**-1.75**	*ns (1.37)*	*ns (1.16)*	*ns (1.1)*	*ns (1.74)*
22	Actin, alpha cardiac muscle 1 and Actin, alpha skeletal muscle	**1.87**	*ns (1.54)*	*ns (1.72)*	*ns (-1.2)*	*ns (-1.08)*
28	Fructose-bisphosphate aldolase A	**1.46**	*ns (1.23)*	*ns (1.14)*	*ns (-1.14)*	*ns (-1.28)*
29	Fructose-bisphosphate aldolase A	**1.5**	*ns (1.26)*	*ns (1.06)*	*ns (-1.18)*	*ns (-1.4)*
33	Triosephosphate isomerase	**1.45**	*ns (1.53)*	*ns (1.17)*	*ns (-1.2)*	*ns (-1.2)*
37	Beta-enolase	**1.6**	*ns (1.24)*	*ns (1.18)*	*ns (-1.29)*	*ns (-1.35)*
38	Beta-enolase	**1.61**	*ns (1.27)*	*ns (1.16)*	*ns (-1.27)*	*ns (-1.39)*
39	Beta-enolase	**1.52**	*ns (1.25)*	*ns (1.2)*	*ns (-1.2)*	*ns (-1.25)*
40	Beta-enolase	**1.47**	*ns (1.17)*	*ns (1.09)*	*ns (-1.25)*	*ns (-1.35)*
42	Fumarate hydratase, mitochondrial	**1.76**	*ns (1.41)*	*ns (1.36)*	*ns (-1.24)*	*ns (-1.17)*
43	Fumarate hydratase, mitochondrial	**1.56**	*ns (1.3)*	*ns (1.27)*	*ns (-1.29)*	*ns (-1.21)*
45	Dihydrolipoyl dehydrogenase, mitochondrial	**1.38**	*ns (1.22)*	*ns (1.31)*	*ns (-1.27)*	*ns (-1.2)*
49	NADH dehydrogenase [ubiquinone] 1 beta subcomplex subunit	**-1.35**	*ns (-1.18)*	*ns (-1.26)*	*ns (1.15)*	*ns (1.07)*
51	ATP synthase subunit alpha, mitochondrial	**I1.7**	*ns (1.51)*	*ns (-1.1)*	*ns (-1.16)*	*ns (-1.95)*
52	Fatty acid-binding protein, heart	**-2.3**	*ns (-1.35)*	*ns (-1.6)*	*ns (1.7)*	*ns (1.4)*
53	Enoyl-CoA hydratase, mitochondrial	**1.46**	*ns (1.28)*	*ns (1.31)*	*ns (-1.21)*	*ns (-1.19)*
56	Creatine kinase M-type	**1.9**	*ns (1.39)*	*ns (1.21)*	*ns (-1.35)*	*ns (-1.56)*
61	Creatine kinase M-type	**1.7**	*ns (1.68)*	*ns (1.41)*	*ns (-1.02)*	*ns (-1.24)*
62	Creatine kinase M-type	**1.5**	*ns (1.67)*	*ns (1.42)*	*ns (-1.02)*	*ns (-1.21)*
66	Creatine kinase M-type	**2.33**	*ns (1.43)*	*ns (1.2)*	*ns (-1.62)*	*ns (-1.93)*
68	Creatine kinase S-type, mitochondrial	**1.5**	*ns (1.35)*	*ns (1.1.18)*	*ns (-1.13)*	*ns (-1.29)*
74	Carbonic anhydrase 3	**1.6**	*ns (1.31)*	*ns (1.4)*	*ns (-1.2)*	*ns (-1.13)*
77	Glyoxylate reductase/hydroxypyruvate reductase	**1.9**	*ns (1.43)*	*ns (1.54)*	*ns (-1.32)*	*ns (-1.23)*
78	Malate dehydrogenase, cytoplasmic	**-1.3**	*ns (-1.04)*	*ns (-1.03)*	*ns (1.24)*	*ns (1.25)*
82	Serotransferrin	**1.5**	*ns (1.27)*	*ns (1.38)*	*ns (-1.16)*	*ns (-1.07)*
84	Serum albumin	**1.87**	*ns (1.68)*	*ns (1.31)*	*ns (-1.06)*	*ns (-1.35)*
88	Voltage-dependent anion-selective channel protein 1	**1.4**	*ns (1.27)*	*ns (1.26)*	*ns (-1.11)*	*ns (-1.12)*
89	MICOS complex subunit Mic60	**1.3**	*ns (1.3)*	*ns (1.31)*	*ns (1.01)*	*ns (1.02)*
91	26S protease regulatory subunit 8	**1.5**	*ns (1.4)*	*ns (1.42)*	*ns (-1.1)*	*ns (-1.09)*
94	Electron transfer flavoprotein subunit alpha, mitochondrial	**1.6**	*ns (1.42)*	*ns (1.2)*	*ns (-1.13)*	*ns (-1.34)*
		Group II				
32	Triosephosphate isomerase	1.56	*ns (-1.06)*	*ns (-1.8)*	**-1.65**	**-1.82**
34	Triosephosphate isomerase	2.1	*ns (1.04)*	*ns (1.15)*	**-2.02**	**-1.81**
55	Creatine kinase M-type	2.4	**1.97**	*ns (1.4)*	ns *(-1.2)*	**-1.71**
63	Creatine kinase M-type	1.6	*ns (1.11)*	*ns (-1.16)*	*ns (-1.42)*	**-1.83**
64	Creatine kinase M-type	1.5	*ns (-1.02)*	*ns (-1.04)*	**-1.51**	**-1.55**
72	Alcohol dehydrogenase [NADP(+)]	1.7	*ns (1.47)*	*ns (1.19)*	*ns (-1.17)*	**-1.45**
		Group III				
1	LIM domain-binding protein 3	**1.52**	*ns (1.5)*	**1.5**	*ns (1.03)*	*ns (1)*
4	LIM domain-binding protein 3	**1.28**	*ns (1.3)*	**1.5**	*ns (1.01)*	*ns (1.04)*
6	Myozenin-1	**1.96**	*ns (1.53)*	**1.6**	*ns (1.07)*	*ns (1.36)*
7	Troponin I, fast skeletal muscle	**1.88**	*ns (1.5)*	**2.2**	*ns (-1.25)*	*ns (1.16)*
9	Troponin I, fast skeletal muscle	**1.58**	*ns (1.4)*	**1.6**	*ns (-1.1)*	*ns (-1.01)*
10	Troponin T, fast skeletal muscle	ns *(1.38)*	*ns (1.22)*	**1.8**	*ns (1)*	*ns (1.33)*
12	Troponin T, fast skeletal muscle	**1.7**	*ns (1.5)*	**1.9**	*ns (-1.1)*	*ns (1.1)*
14	Myosin regulatory light chain 2, skeletal muscle isoform	**-1.83**	**-2**	*ns (-1.2)*	*ns (-1.13)*	*ns (1.24)*
19	Myosin light chain 1/3, skeletal muscle isoform	ns *(-1.6)*	**-4.9**	*ns (-2)*	*ns (-2.01)*	*ns (-1.3)*
20	Myosin light chain 1/3, skeletal muscle isoform	**-2.1**	**-2**	*ns (-1.5)*	*ns (1.'04)*	*ns (1.'35)*
27	Myotilin	*ns (1.35)*	*ns (1.41)*	**1.56**	*ns (1.05)*	*ns (1.15)*

31	Fructose-bisphosphate aldolase A	**1.69**	**1.68**	*ns (1.51)*	*ns (1.)*	*ns (-1.1)*
36	Triosephosphate isomerase	*ns (1.13)*	*ns (-1.43)*	*ns (-1.43)*	**-1.9**	**-1.89**
41	UTP--glucose-1-phosphate uridylyltransferase	**1.56**	**1.37**	ns *(1.34)*	ns *(-1.14)*	ns *(-1.14)*
44	Malate dehydrogenase, mitochondrial	**1.73**	**1.7**	*ns (1.6)*	*ns (-1.25)*	*ns (-1.25)*
47	Aconitate hydratase, mitochondrial	*ns (1.14)*	**1.5**	*ns (1.16)*	*ns (1.34)*	*ns (1.02)*
48	NADH dehydrogenase [ubiquinone] flavoprotein 2, mitochondrial	*ns (1.35)*	ns *(-1.38)*	*ns (-1.38)*	**-1.9**	**-1.9**
54	Succinyl-CoA:3-ketoacid coenzyme A transferase 1, mitochondrial	**1.5**	ns *(1.33)*	**1.4**	ns *(-1.13)*	ns *(-1.08)*
57	Creatine kinase M-type	**1.5**	**2.83**	*ns (2.2)*	*ns (1.05)*	*ns (1.22)*
58	Creatine kinase M-type	**2.1**	**2.3**	*ns (1.8)*	*ns (1.11)*	*ns (-1.12)*
59	Creatine kinase M-type	**-1.9**	**-1.46**	*ns (-1.35)*	*ns (1.29)*	*ns (1.47)*
60	Creatine kinase M-type	**2.4**	**2.3**	*ns (1.7)*	*ns (-1.02)*	*ns (-1.35)*
67	Creatine kinase M-type	**1.3**	ns *(1.15)*	**1.4**	ns *(-1.14)*	ns *(1.09)*
75	Carbonic anhydrase 3	**1.5**	**1.35**	*ns (1.24)*	*ns (-1.27)*	*ns (-1.35)*
80	Hemoglobin subunit beta-1	*ns (1.01)*	**-1.3**	**-1.4**	*ns (-1.98)*	*ns (-2.1)*
86	Serum albumin	**-1.3**	**-1.4**	**-1.63**	*ns (-1.07)*	*ns (-1.26)*
87	Voltage-dependent anion-selective channel protein 1	**1.4**	**1.41**	*ns (1.31)*	*ns (1)*	*ns (-1.07)*
95	Heat shock protein beta-1	*ns (1.13)*	*ns (-1.34)*	*ns (-1.5)*	*ns (-1.5)*	**-1.68**

¤ Significant fold changes are reported in bold; *ns* means not significant, the corresponding fold changes values are in italics between brackets and are reported in order to show the tendency.
*Fold change mdx exe *vs* mdx as reported in Table 3.

łFold change mdx apo and mdx tau *vs* mdx.

≠Fold change mdx apo and mdx tau *vs* mdx exe.

Figure Legends

Figure 1. Representative silver-stained 2DE gel image of tibialis anterior muscle from mdx mice. Proteins (70 µg) were separated by 2DE using IPG strips with a nonlinear pH gradient of 3–10 and 9–16% linear gradient SDS-PAGE. Circles and numbers indicate statistically differentially abundant proteins between the five groups analysed. Numbers correspond to the spot numbers present in Table 1.

Figure 2. PCA biplot. Red circle includes spots of gels from mdx (pink dots) and wt (light blue dots); blue circle includes spots of gels from mdx exe (blue dots) and mdx exe treated with apocynin (violet dots) and taurine (yellow dots).

Figure 3. Over-representation enrichment analysis (ORA): enriched gene ontology categories (A) and pathway (B). Statistical enrichment was performed using WebGestalt web tool (http://webgestalt.org). R: ratio of enrichment; adjP: p value adjusted by the multiple test adjustment. Only categories with an adjP ≤ 0.05 are reported.

Figure 4. Overview of 2DE results. Impact of exercise on proteins involved in sarcomere structure and muscle contraction. (*) indicates proteins whose Mr or/and pI were different than expected.

Figure 5. Validation of proteomic results. Histograms and representative immunoblot images of Actin (panel A) and Aldoa, Tpi1 and Eno3 (panel B) from mdx and mdx exe mice. (n=5; mean ± S.D.; t-test unpaired). Normalization of immunoblot was performed on Coomassie stained gel as described in Materials and Methods.

Figure 6. Immunoblot of electron chain complexes with total OXPHOS Rodent WB Antibody Cocktail. Histograms and representative immunoblot images from mdx and mdx exe mice. (n=5; mean ± S.D.; t-test unpaired). Normalization of immunoblot was performed on Coomassie stained

membrane as described in Materials and Methods. Complex IV is visible only with prolonged exposition (not shown).

Figure 7. Impact of exercise on proteins involved in glucose metabolism, TCA cycle and electron transport chain. Protein variation found by 2DE are represented inside the squares. Protein variations of each complex, arising from OXPHOS western blot analysis, are indicated in bold.

Figure 8. Immunoblotting of exercise-related proteins. Histograms and representative immunoblot images of Sirt1 and PGC1-alpha in wt, mdx and mdx exe mice. (n=5; mean ± S.D.; one–way ANOVA). Normalization of immunoblot was performed on Coomassie stained gel as described in Materials and Methods

Figure 9. Clustering representation of the three groups obtained considering treatments effect. Group I: spots whose abundance were modified by exercise, but that, with taurine and/or apocynin treatment, showed a reduction of this modification that became non-significant. Group II: spots that show a significant variation between mdx exe and mdx exe treated with compounds. Group III spots that behave in intermediates ways between the two previous groups.

Figure

Click here to download high resolution image

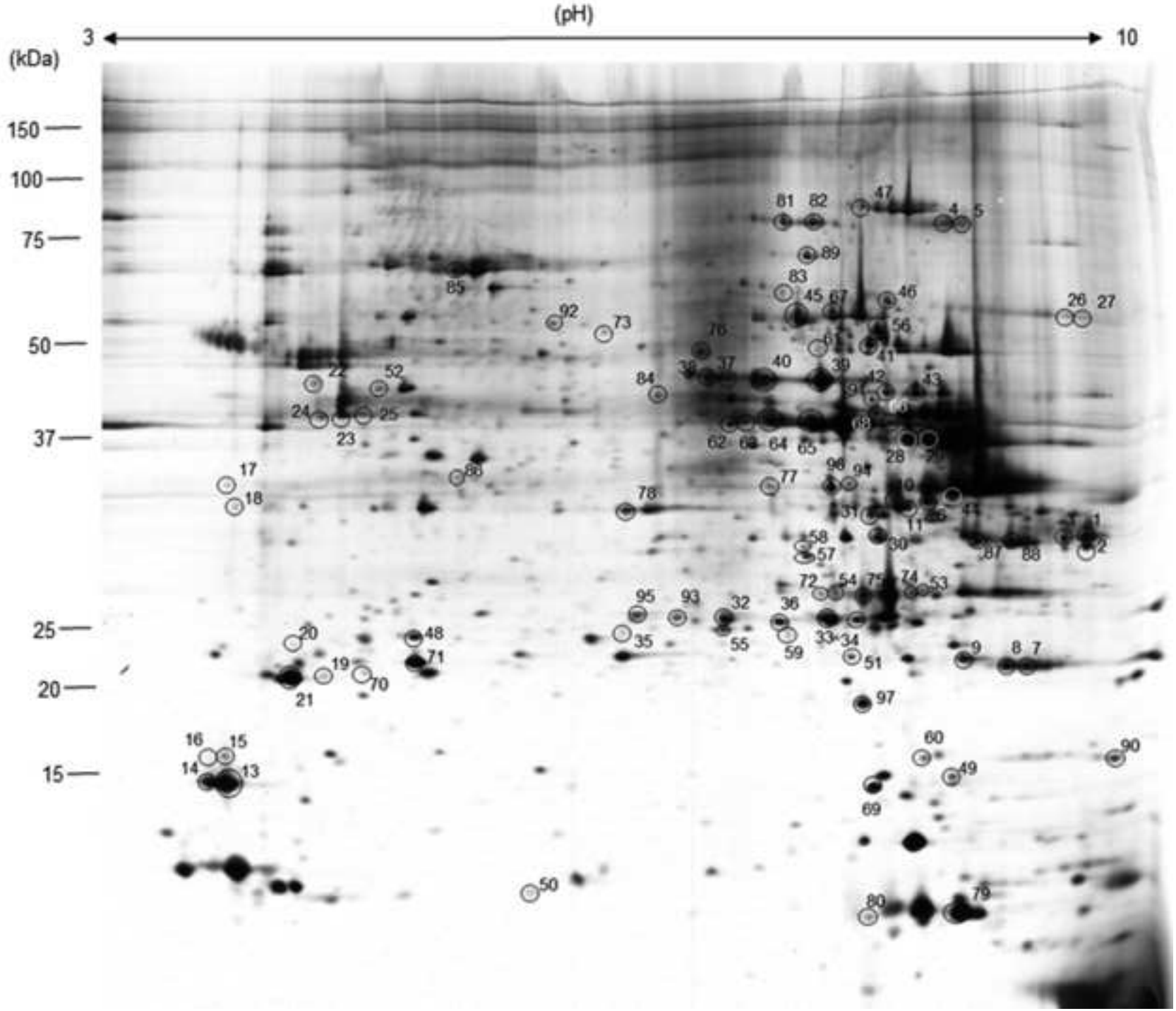

Figure

Click here to download high resolution image

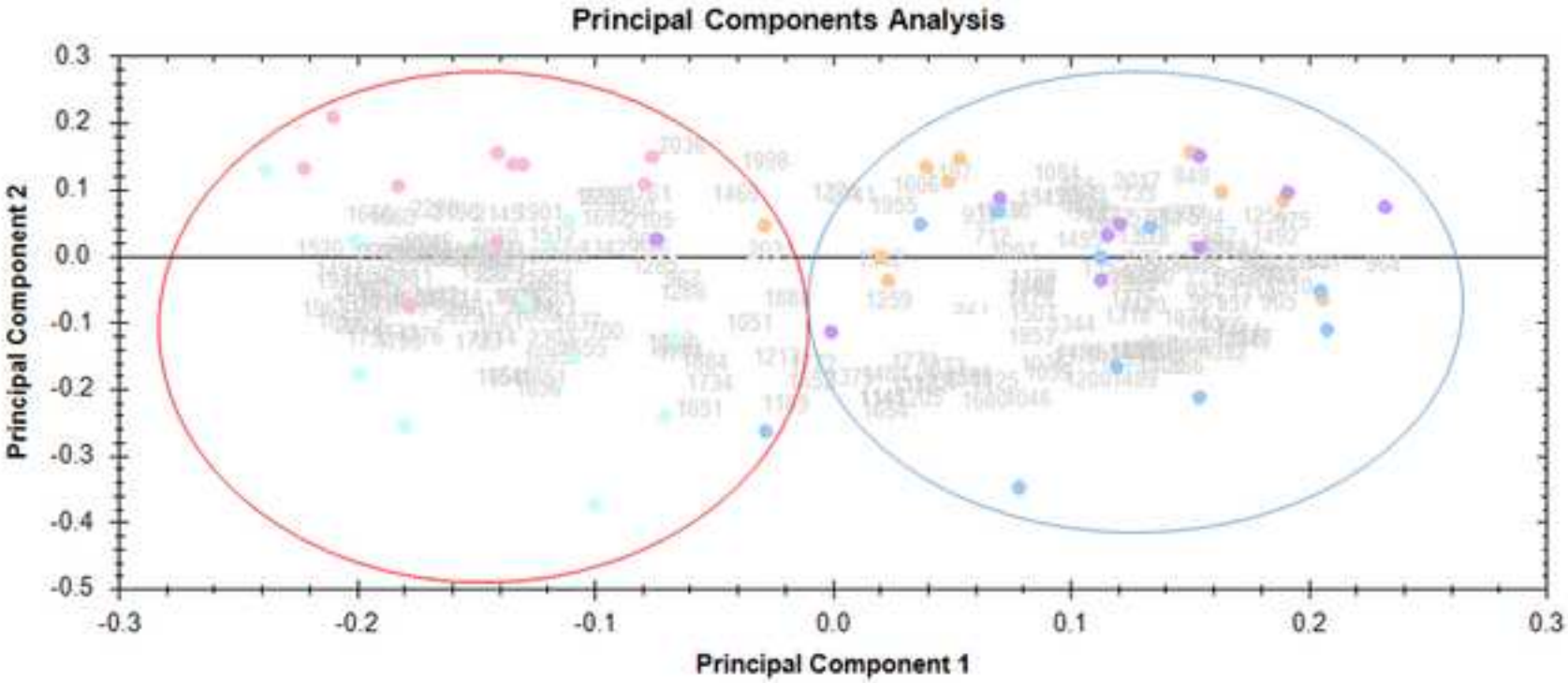

Figure

Click here to download high resolution image

Enriched biological process categories	adjP
Dicarboxylic acid metabolic process (GO:0043648)	6.09E-05
Pyridine-containing compound metabolic process (GO:0072524)	1.69E-04
Generation of precursor metabolites and energy (GO:0006091)	1.69E-04
Nucleoside triphosphate metabolic process (GO:0009141)	2.83E-04
Nucleotide phosphorylation (GO:0046939)	2.83E-04
Cellular component assembly involved in morphogenesis (GO:0010927)	3.72E-04
Nucleoside diphosphate metabolic process (GO:0009132)	5.87E-04
Glycosyl compound metabolic process (GO:1901657)	1.24E-03
Nucleoside monophosphate metabolic process (GO:0009123)	2.60E-03
Actomyosin structure organization (GO:0031032)	3.58E-03
Enriched cellular component categories	
Blood microparticle (GO:0072562)	0.0006
Actin cytoskeleton (GO:0015629)	0.0007
Mitochondrial matrix (GO:0005759)	0.0007
Mitochondrial protein complex (GO:0098798)	0.0166
Organelle inner membrane (GO:0019866)	0.0392
Enriched molecular function categories	
Lyase activity (GO:0016829)	0.014
Oxidoreductase activity, acting on CH-OH group of donors (GO:0016614)	0.0335
Cofactor binding (GO:0048037)	0.0335

A

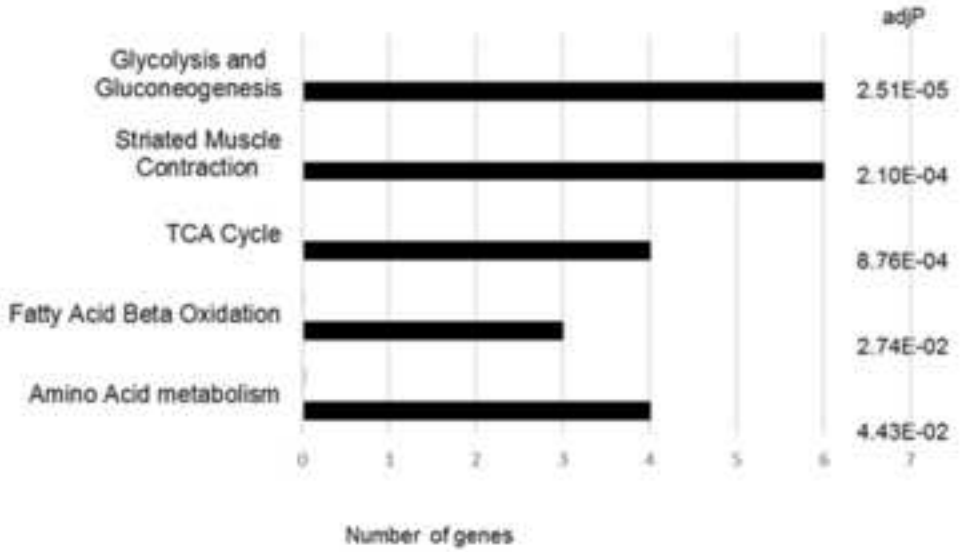

B

Figure

Click here to download high resolution image

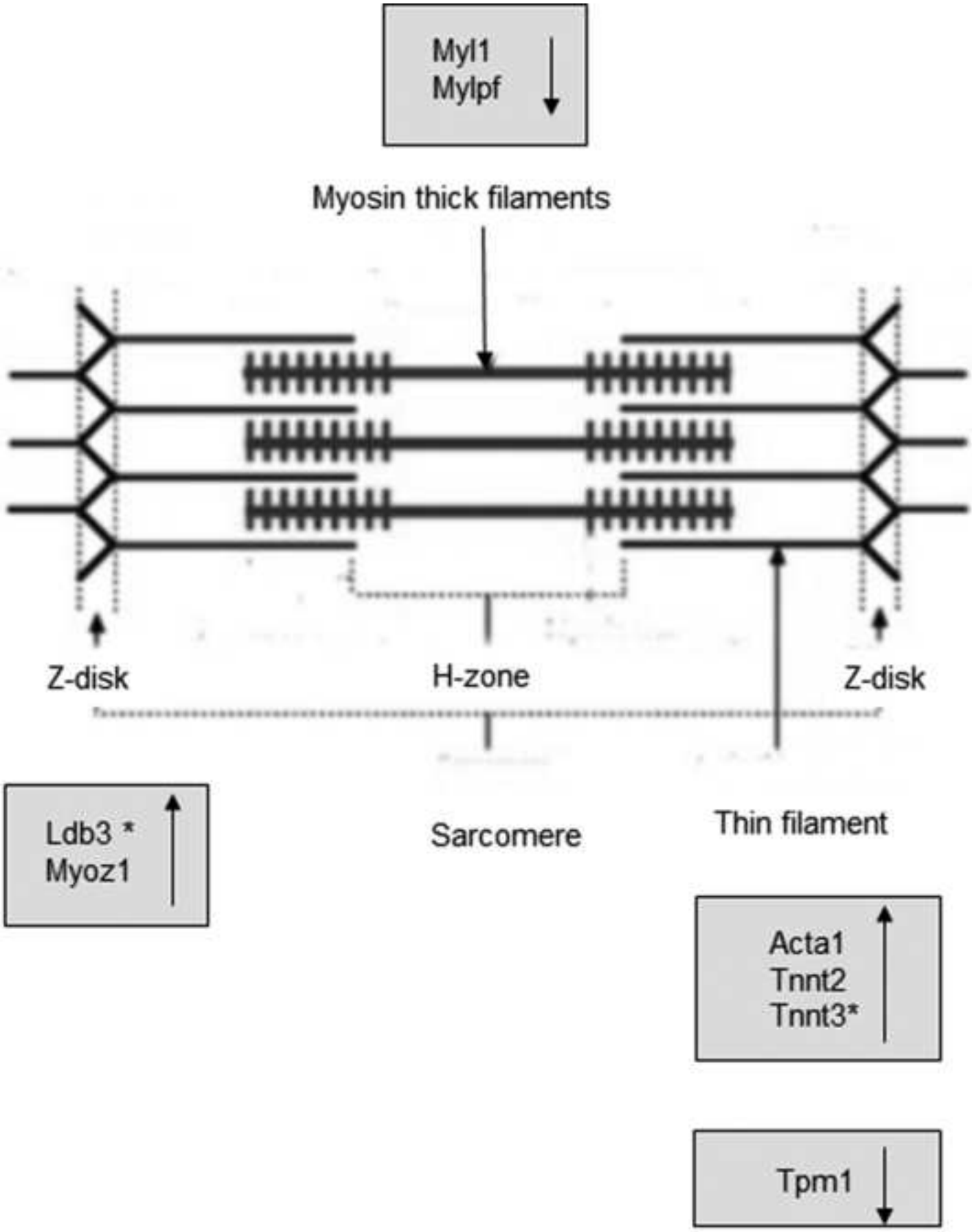

Figure

Click here to download high resolution image

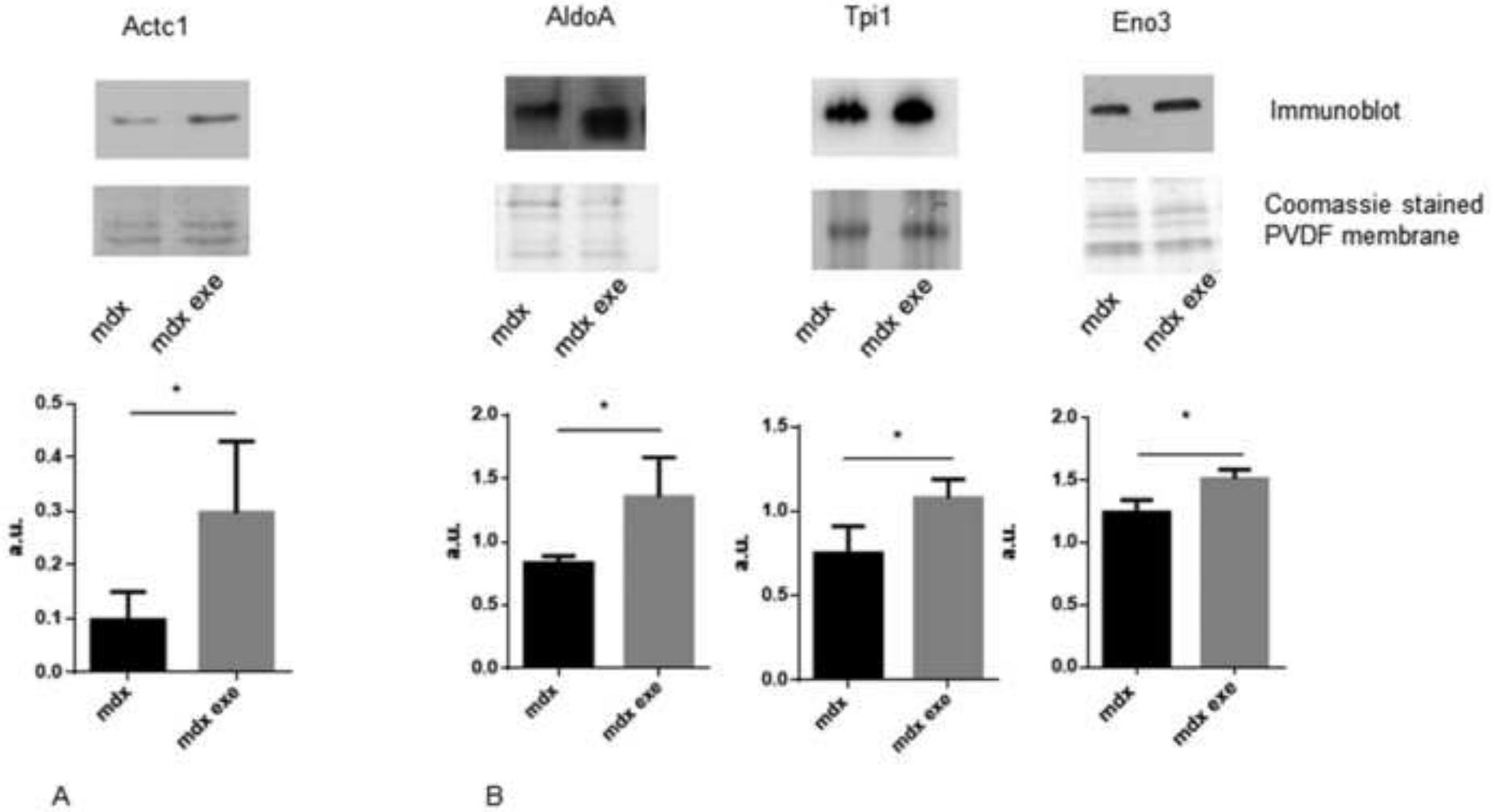

Figure

Click here to download high resolution image

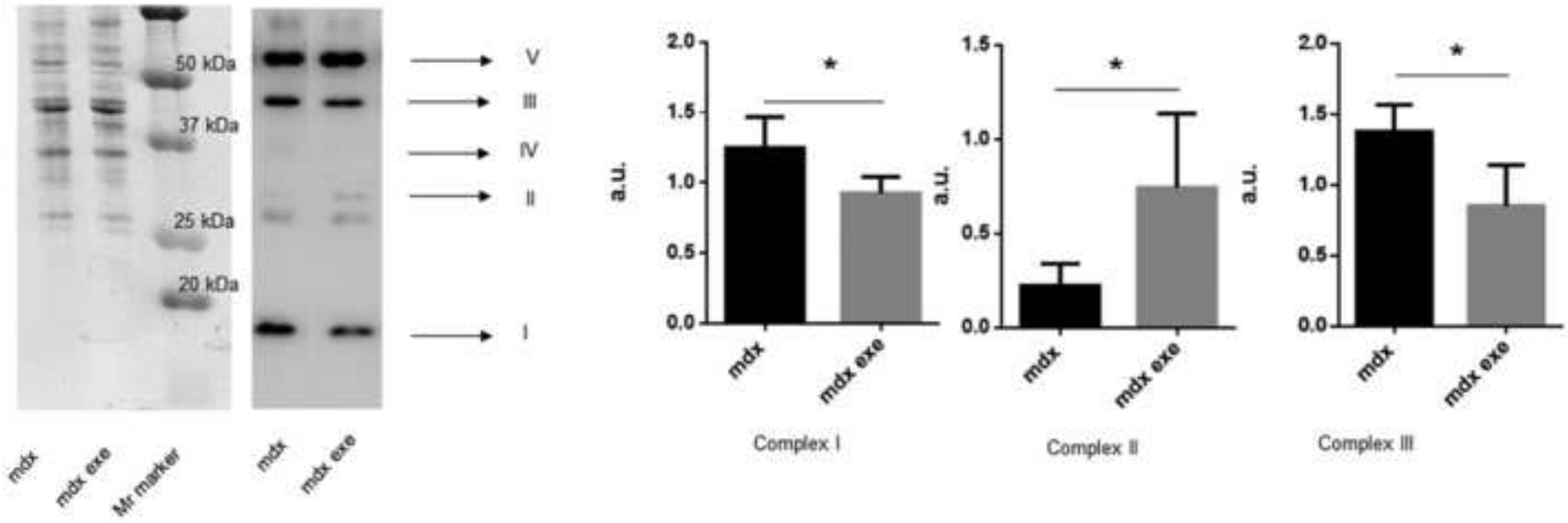

Figure

Click here to download high resolution image

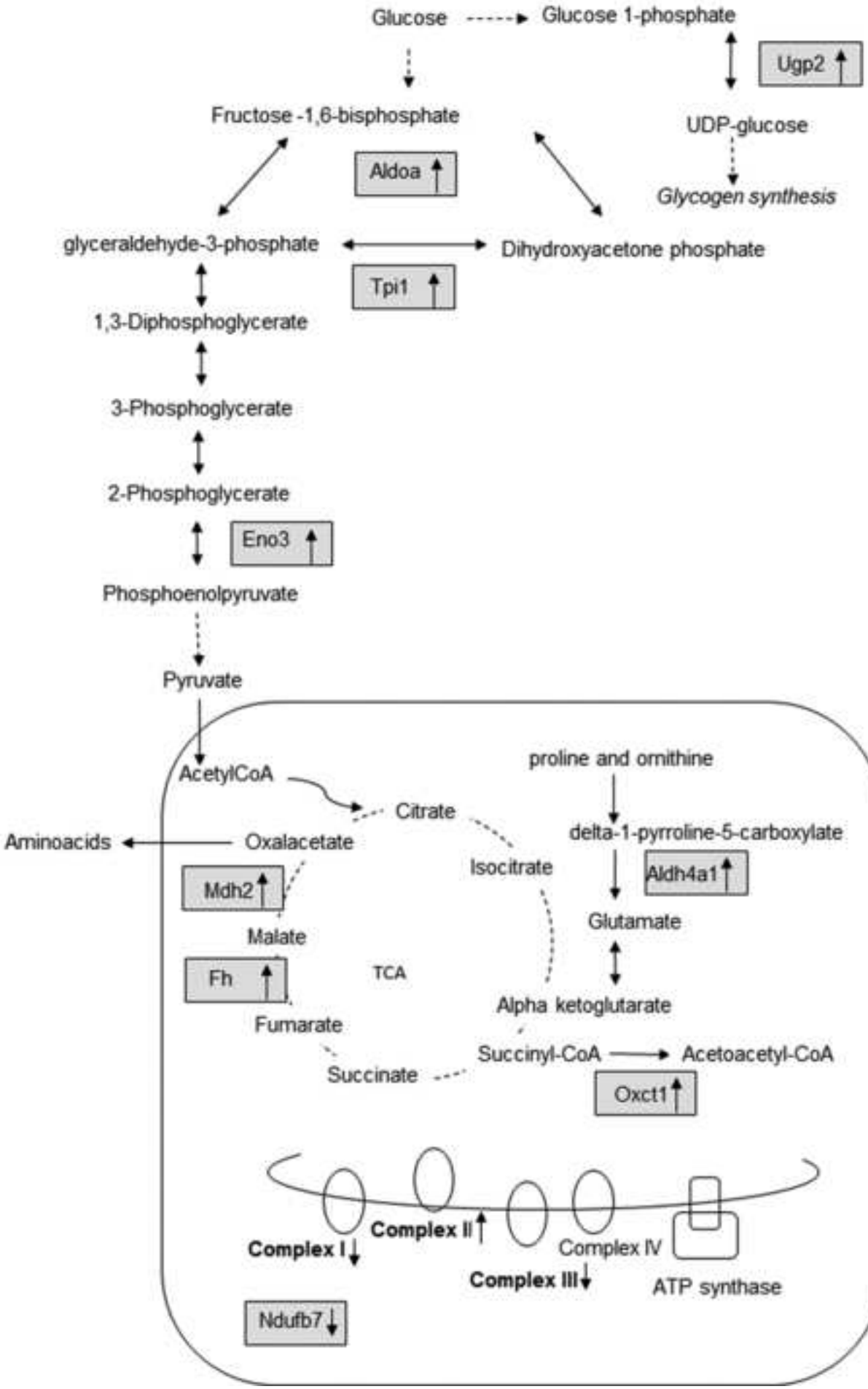

Figure
Click here to download high resolution image

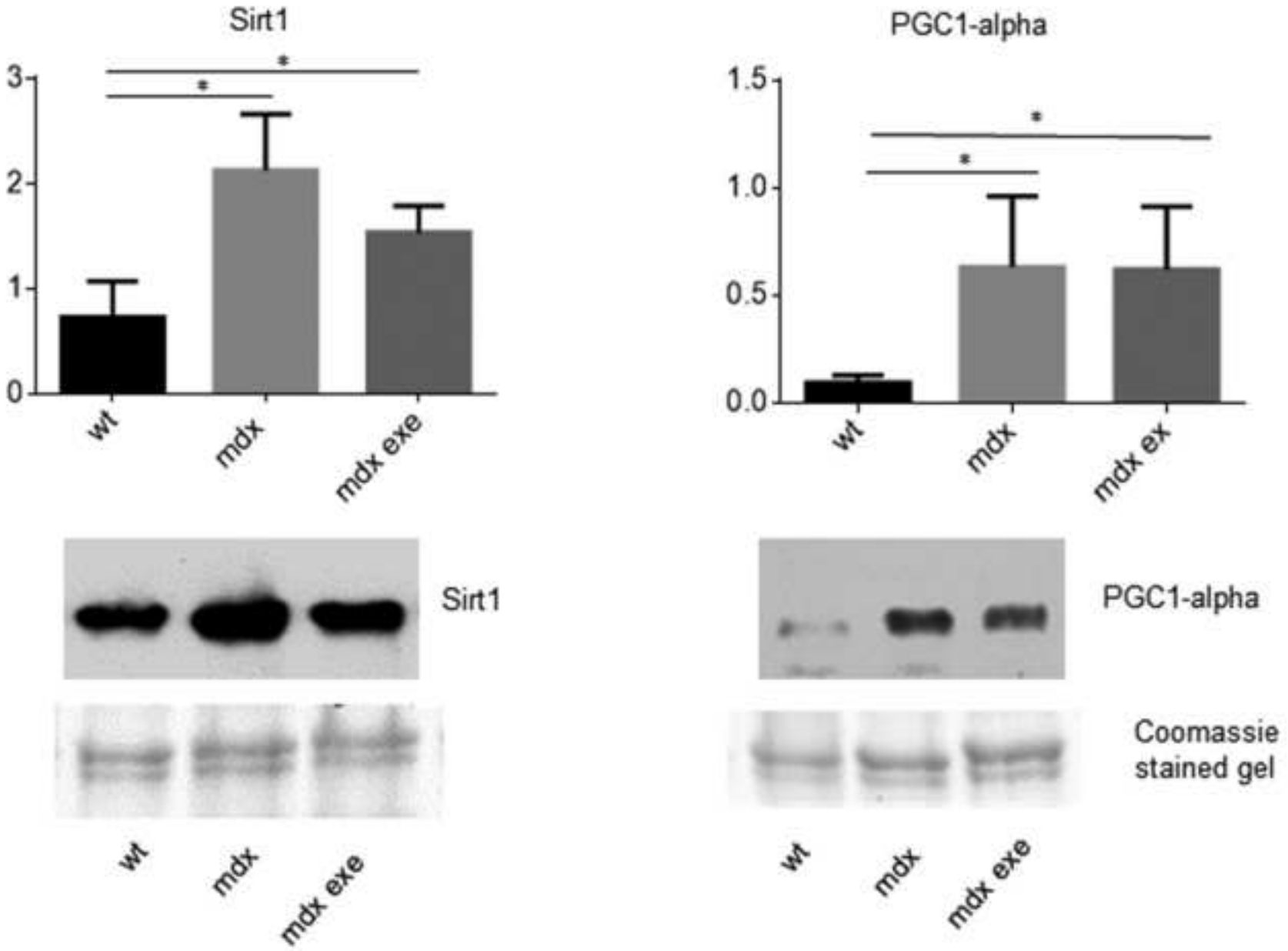

Figure

Click here to download high resolution image

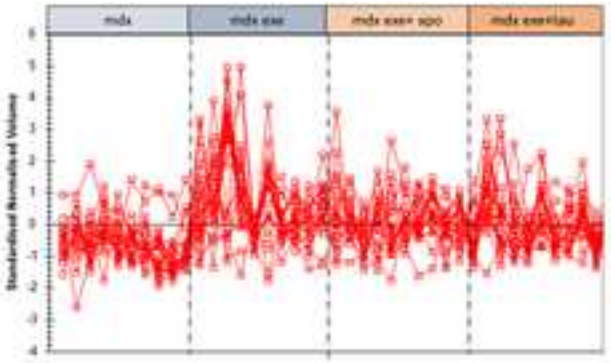

Group I

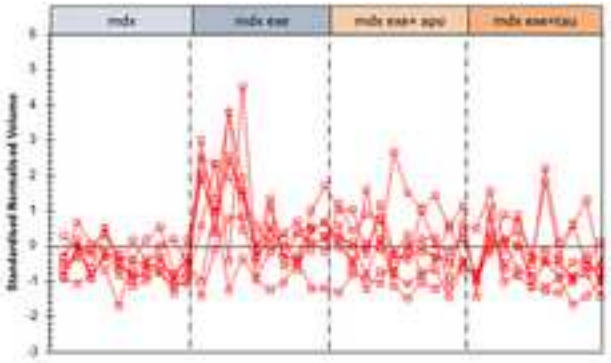

Group II

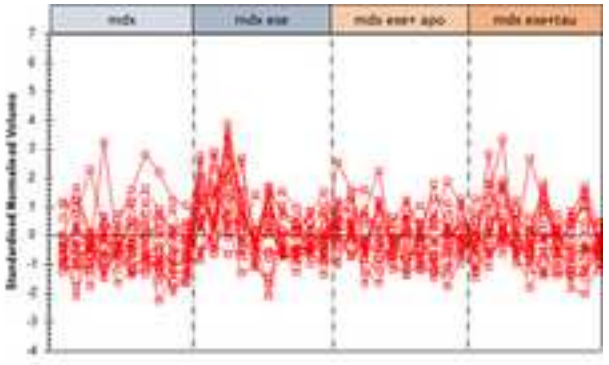

Group III

***Conflict of Interest**

Click here to download Conflict of Interest: coi_disclosure.pdf

Data in Brief

Click here to download Data in Brief: Data in brief article.zip